

Entanglement in quantum bit cloning and in Hardy's paradox

Levente Szabó

supervisor:

Mátyás Koniorczyk

A dissertation

submitted in partial satisfaction of the requirements for the degree

Doctor of Philosophy

in physics



University of Pécs

Doctoral School of Physics

Doctoral Program of Quantum Optics

2017.

"Everything we call real is made of things that cannot be regarded as real."

Niels Bohr

Contents

Introduction	4
1 Background and notation	6
1.1 Systems and states	6
1.1.1 Physical transformations of states	8
1.2 Quantum entanglement	10
1.2.1 Mixed state entanglement	12
1.2.2 The Wootters formula	13
1.2.3 Entanglement of multi-qubits systems	14
1.2.4 Monogamy of entanglement	15
1.3 Quantum cloning	16
1.4 Interaction-free measurement	18
1.5 Hardy's paradox	21
2 Optimal universal asymmetric covariant quantum cloning circuits for qubit entanglement manipulation	25

2.1	Bipartite pure states	27
2.2	The GHZ state	32
2.3	Conclusion	36
3	Hardy's paradox and the entanglementlike structure of forward-scattered waves	39
3.1	The setup	39
3.2	Forward scattering	41
3.3	Conclusion	44
4	Forward-scattered wave analysis of an optical Hardy-like setup	45
4.1	The optical Hardy-like setup	46
4.2	Forward scattering	50
4.3	Conclusion	52
5	Summary	53
6	Összefoglalás	
	(Summary in Hungarian)	56
	List of related publications	59
	Acknowledgements	60
	Bibliography	61

Introduction

Quantum mechanics is the fundamental theory of all modern physics. As such it is a significant part of our understanding of Nature. It employs sophisticated mathematical models whose interpretation still poses unresolved physical and philosophical questions. Some of these lead to phenomena which are unusual and counterintuitive from an everyday perspective. In spite of this, quantum mechanics is a very successful theory. While its grounding fathers considered it as a theory for multipartite systems not verifiable on the level of individual physical systems, the formidable development of experimental technology (especially that of quantum optics) in the last decades has made the direct observation of these counterintuitive phenomena viable. And indeed: quantum mechanics appears to be valid for individual physical systems.

Moreover, the accessibility of quantum phenomena seems to find its way to practical applications. The paradigm shift in physics introduced by quantum mechanics seems to be repeated in the field of information theory and information processing: quantum information now has a well-established reputation amongst future and emerging technologies. While quantum random generators and some quantum ciphers are commercial products already, yet there are still a lot of details to be better understood.

The present dissertation describes my results which contribute mainly to the field of quantum information. In this field, quantum cloning is considered as an important information processing primitive. I have studied the interrelations of cloned quantum bits to a rest of the quantum system their originals belong to, in the case of a particular quantum cloner design. As quantum information science is often deeply related to the fundamental aspects of quantum mechanics. These aspects sometimes lead to

paradoxical consequences when viewed from a classical physical perspective. My other aim was to better understand some details of such a paradox, introduced by Hardy.

The dissertation itself is based on results which appeared in three independent publications. The topics may seem to be diverse, however, there is a key concept which interrelates all the presented results, namely *quantum entanglement*.

Chapter 1

Background and notation

In this Chapter we summarize the notation and the scientific context of my results. Section 1.1 is devoted to the description of the very concepts in quantum mechanics used in this study. In Section 1.2 we briefly introduce those elements of quantum entanglement theory we will use. These Sections are there for the sake of completeness and to introduce the notation, there is no intention to give a full introduction to these broad topics. With this respect we refer to the extensive literature of the field. The following three Sections deal with the phenomena we have actually studied in order to put my results into their scientific context. A brief summary of the topic of quantum cloning can be found in Section 1.3. In Section 1.4 we give a short guide to the topic of the interaction-free measurement. Finally, in Section 1.5 we outline the playground of Hardy's paradox and some other ideas related to it.

1.1 Systems and states

A quantum system is modeled by a separable Hilbert space \mathcal{H} . In the present work we deal only with systems whose Hilbert space is finite dimensional. We use Dirac's notation: the vectors are the *kets*,

$$|\Psi\rangle \in \mathcal{H}, \tag{1.1}$$

while the elements of the dual of \mathcal{H} are the *bras*:

$$\langle \Psi | \in \mathcal{H}^*, \quad (1.2)$$

thus the scalar product of the vectors $|\Psi\rangle$ and $|\Phi\rangle$ reads

$$\langle \Phi | \Psi \rangle = \langle \Psi | \Phi \rangle^*. \quad (1.3)$$

We frequently use orthonormal bases in our considerations. For a two-dimensional system (that is, a quantum bit), for instance, we have

$$\begin{aligned} \mathcal{H} &= \text{span}(|0\rangle, |1\rangle) \\ \langle i | j \rangle &= \delta_{ij}, \quad i, j \in \{0, 1\}, \end{aligned} \quad (1.4)$$

where δ_{ij} is the Kronecker delta symbol. Systems with two dimensional Hilbert spaces can be and are realized in experiments. The possible realizations include: spins of electrons, polarization of single photons, circular Rydberg atoms, etc.

When dealing with multipartite systems, each subsystem has its own Hilbert space. The whole system lives in the tensor product of the spaces. For two quantum bits, for instance, we have

$$\mathcal{H} = \mathcal{H}_1 \otimes \mathcal{H}_2 = \text{span}(|0\rangle_1 \otimes |0\rangle_2, |0\rangle_1 \otimes |1\rangle_2, |1\rangle_1 \otimes |0\rangle_2, |1\rangle_1 \otimes |1\rangle_2). \quad (1.5)$$

In what follows we omit the \otimes symbol in states and we write $|\Psi\rangle_1 |\Phi\rangle_2$ or $|\Psi_1 \Phi_2\rangle$ instead of $|\Psi\rangle_1 \otimes |\Phi\rangle_2$. The maybe most intriguing feature of quantum systems, quantum entanglement, stems from the fact that not all elements of the product space are products of individual subsystems. We return to this point in Section 1.2.

Quantum states described by vectors of the Hilbert space are referred to as *pure states*. In the case when we do not exactly know the state of the system, but at least we have a prior information that with probability p_i it is in a state $|\Psi_i\rangle$, its state is described by a density operator which is a convex combination of projectors:

$$\varrho = \sum_i p_i |\Psi_i\rangle \langle \Psi_i|. \quad (1.6)$$

Note that here i can be an element of an arbitrary index set (possibly even infinite, but we deal with finite ones here), and there is no restriction on the states $|\Psi_i\rangle$. The set of density operators of a system is a convex set of unit trace Hermitian positive semidefinite operators. The extremal states are the pure states, they are rank one projectors. Also note that the form of a density operator in Eq. (1.6) is not unique: different sets of states and different probabilities can yield the same density operator. This ambiguity lies in the very heart of the difference between classical probabilistic systems and quantum ones: the description of the state as a convex combination of the extremal states is ambiguous in the latter case.

Returning to multipartite systems, if the multipartite system is in a given quantum state (mixed, ρ or pure $\rho = |\Psi\rangle\langle\Psi|$), the state of a subsystem is its partial trace, which can be expressed on an arbitrary product basis (c.f. Eq. (1.5)) as

$$\rho_{i,j}^{(1)} = [\text{Tr}_2 \rho]_{i,j} = \sum_k \rho_{ik|jk}, \quad (1.7)$$

where $\rho_{ik|jk} = \langle ik | \rho | jk \rangle$.

1.1.1 Physical transformations of states

Unitaries

Time evolution, as described by the Schrödinger equation, results in a unitary transformation of the state:

$$|\Psi'\rangle = U |\Psi\rangle, \quad U^\dagger U = \hat{I}, \quad (1.8)$$

(\hat{I} stands for the identity operator while \dagger for Hermitian conjugation), whereas for mixed states we have

$$\rho' = U \rho U^\dagger. \quad (1.9)$$

Note that we do not refer to time in the last two equations: in topics of quantum information, unitaries are typically considered as physically feasible transformations of quantum states without going into details of the actual interaction and time to realize them. They are also referred to as *quantum gates*.

Projective measurements and beyond

Measurables in quantum mechanics are modeled by Hermitian operators, which can be given in general in terms of their eigenvalues $m \in \mathbb{R}$ and the corresponding eigenvectors $|m\rangle$:

$$\hat{M} = \sum_m m |m\rangle \langle m| \quad (1.10)$$

Note that the states $|m\rangle$ form a basis on the Hilbert-space of the system. Were the spectrum of \hat{M} degenerate, we can always choose orthogonal states in the eigensubspace (e.g. via Gram-Smith orthogonalization), so we always have a basis of eigenstates, albeit with some ambiguity in the degenerate case.

When the measurement is carried out on a system in state $|\Psi\rangle$, the apparatus displays the result m with the probability

$$p_m = |\langle m|\Psi\rangle|^2. \quad (1.11)$$

Here we encounter yet another (if not the most) intriguing feature of quantum mechanics: right after the measurement the system is left in state $|m\rangle$ and the state $|\Psi\rangle$ is destroyed. This is not only the basis of many physical and philosophical disputes (including the Einstein-Podolsky-Rosen paradox), but also leads to experimentally testable consequences such as the quantum Zeno effect. Moreover, one can make use of this feature: quantum cryptography would be impossible without entanglement.

In the degenerate case the state is projected into an eigensubspace corresponding to the given measurement result. When measuring mixed states, the measurement probabilities are the diagonal elements of the density operator expanded in the measurable's eigenbasis. In case of a nondegenerate measurement, the state will be in the corresponding eigenstate of the measurement. (Note that it is actually pure in this case, too.)

We briefly mention that there are more general measurements feasible in quantum systems. They can be realized by projectively measuring a larger system whose subsystem is the one to be measured. These are referred to as POVM measurements, but we do not use them in our work.

Completely positive maps

As we have to discuss cloning we have to briefly mention completely positive maps. They are the most general transformations which can be realized on a physical system:

$$\varrho' = \mathcal{E}(\varrho) \quad (1.12)$$

The transformation \mathcal{E} has to be linear, trace preserving and it should also be positive (that is, preserve the positive semidefiniteness of the density operator). However, there is another important requirement: it should be *completely positive*: if the system is supplemented by any other system, say, with a Hilbert space \mathcal{H}' whose identity operator is \hat{I} , the (super)operator $\mathcal{E} \otimes \hat{I}$ should be also positive. The reason behind this is: if we perform the operation on a system while we do nothing with any ancillary system, then the resulting state of our system and the ancilla has to be still positive.

There exist positive but not completely positive operators. An important example is the transposition in an orthonormal basis, which plays an important role in the theory of quantum entanglement.

1.2 Quantum entanglement

Let us return to quantum entanglement and outline its aspects which are relevant for our work. We say that the quantum state $|\Psi\rangle \in \mathcal{H}_1 \otimes \mathcal{H}_2$ of a bipartite system is *separable* if it is a product of states of each subsystem:

$$|\Psi\rangle = |\Psi_1\rangle |\Psi_2\rangle, \quad |\Psi\rangle_1 \in \mathcal{H}_1, \quad |\Psi\rangle_2 \in \mathcal{H}_2. \quad (1.13)$$

If a state is not separable, it is *entangled*.

The definition can be obviously extended to multipartite systems. And as we shall see later, the entanglement of multipartite systems bears a rich structure.

If a pure state $|\Psi\rangle$ is separable, then all the subsystems are in a pure state. Thus their density operators are projectors. E.g. for

$$\varrho^{(1)} = \text{Tr}_2 |\Psi\rangle \langle\Psi| \quad (1.14)$$

we have

$$(\varrho^{(1)})^2 = \varrho. \quad (1.15)$$

As $\text{Tr } \varrho = 1$, it implies that

$$\text{Tr } (\varrho^{(1)})^2 = 1. \quad (1.16)$$

This holds for all the subsystems if and only if the state is separable.

Considering a bipartite system this leads to a possibility of quantifying entanglement: the “more mixed” a subsystem is, the more entangled the state is. The mixedness of the state is commonly measured by the von Neumann entropy of the density operator

$$H(\varrho) = -\text{Tr}(\varrho \log_2 \varrho), \quad (1.17)$$

which bears a sound information theoretic interpretation. In a d -dimensional system its maximum value is $\log_2 d$, attained by the state

$$\varrho_{\text{CM}} = \frac{1}{d} \hat{I}. \quad (1.18)$$

This is termed as the completely mixed state. It is the only state which produces a uniform distribution of measurement results when measured in any possible basis. For reasons not detailed here the partial traces of a pure bipartite state have the same von Neumann entropy. Hence it is reasonable to say that the *entanglement* of the state is quantified by

$$E(|\Psi\rangle) = H(\text{Tr}_2 |\Psi\rangle \langle \Psi|) \quad (1.19)$$

For practical reasons it is worth mentioning that a mathematically simpler quantity can also be used to quantify the mixedness of the state, and thus entanglement, albeit without an operational or direct information theoretic meaning. Its construction stems from the fact that Eq. (1.16) holds if the state is pure. As the diagonal elements of the density matrix describe a probability distributions, for mixed states we have

$$\text{Tr } \varrho^2 < 1. \quad (1.20)$$

Hence, the trace of the square of the density matrix is related to the purity of the state in a way. It can be shown that its minimum value is $1/d$ attained by the completely mixed state only. For quantum

bits (i.e. $d = 2$ we can thus construct a quantity with in the $[0, 1]$ range (just like the von Neuman entropy):

$$H_{\text{lin}}(\varrho) = 2 \left(\frac{1}{2} - \varrho^2 \right). \quad (1.21)$$

This is termed as the *linear entropy* of the state. It can be easily verified that the von Neumann entropy is a monotone function of the linear entropy, and so that of its square root. Hence, entanglement can be described also in terms of concurrence

$$C(|\Psi\rangle) = \sqrt{H_{\text{lin}}(\text{Tr}_2 |\Psi\rangle \langle \Psi|)}. \quad (1.22)$$

The entanglement in Eq. (1.19) is its monotone function in the same range, it can be evaluated with less effort, but does not admit an operational interpretation.

1.2.1 Mixed state entanglement

If a multipartite system is in a mixed state, its entanglement properties are far more complex. As for the definition, a mixed state is said to be a separable one, if it can be constructed as a convex combination of separable pure states or – in other words – it has a form like (1.6) in which every $|\Psi_i\rangle$ is separable. Unseparable mixed states are called entangled.

In many cases it is hard even to decide if a state is separable or entangled at all: obviously in this case the subsystems of a separable state may well be mixed. (Consider the complete mixture of two qubits as an example. It is obviously separable (the density operator being proportional the equal-weight convex combination of the projectors of an arbitrary orthonormal basis, including any product-state basis). Both subsystems are in a completely mixed state though.) Also, while pure-state entanglement is fully characterized by the quantity in Eq. (1.19), for mixed states there are several similar quantities which coincide for pure states but they have different operational meanings otherwise.

One of them is *entanglement of formation* defined as follows:

$$E(\varrho) = \inf_{\substack{(p_k, |\psi_k\rangle \text{ separable}) \\ \sum_k p_k |\psi_k\rangle \langle \psi_k| = \varrho}} \sum_k p_k E(|\psi_k\rangle), \quad (1.23)$$

that is, the infimum of the average of the entanglements of all the constituent pure states over all of its pure-state decompositions. As we deal with finite dimensional states, the infimum can be understood as minimum.

A similar quantity can be defined via concurrence:

$$C(\varrho) = \inf_{\substack{(p_k, |\psi_k\rangle \text{ separable}) \\ \sum_k p_k |\psi_k\rangle\langle\psi_k| = \varrho}} \sum_k p_k C(|\psi_k\rangle), \quad (1.24)$$

It can be shown that entanglement of formation is its monotone function, and in the special case of two qubits it can be calculated analytically. This is the celebrated Wootters formula which is very broadly used in the literature, including our work. Hence we describe it in what follows. For the detailed derivations we refer to the original papers

1.2.2 The Wootters formula

In order to calculate the concurrence of a two-qubit state ϱ , first we define the Wootters tilde operation:

$$\tilde{\varrho} = (\sigma_y \otimes \sigma_y) \varrho^* (\sigma_y \otimes \sigma_y), \quad (1.25)$$

where $*$ means the complex conjugation (or, otherwise speaking, the transpose) of the density matrix in a product state basis, whereas σ_y is the second Pauli-operator.

Next the spectrum of the Hermitian operator has to be determined

$$\sqrt{\sqrt{\varrho} \tilde{\varrho} \sqrt{\varrho}}. \quad (1.26)$$

Its eigenvalues λ are in fact the square roots of the eigenvalues of the (non-Hermitian) operator

$$\varrho \tilde{\varrho}. \quad (1.27)$$

Let us put the eigenvalues $\lambda_1, \lambda_2, \lambda_3, \lambda_4$ to decreasing order. The concurrence then reads

$$C(\varrho) = \max\{0, \lambda_1 - \lambda_2 - \lambda_3 - \lambda_4\} \quad (1.28)$$

We shall employ this latter formula when calculating concurrence throughout this thesis.

1.2.3 Entanglement of multi-qubits systems

It may be an interesting question how can be featured the entanglement of two chosen quantum bits in a system consisting of N quantum bits, if the whole system is in a pure state. As an illustration, let us consider the following specific example: we have three quantum bits in a state which is called Greenberger-Horne-Zeilinger (GHZ) state:

$$|\Psi_{\text{GHZ}}\rangle_{123} = \frac{1}{\sqrt{2}}(|000\rangle + |111\rangle). \quad (1.29)$$

In this case, the state of the first two quantum bits is describes by the density operator

$$\rho_{12} = \frac{1}{2}(|00\rangle\langle 00| + |11\rangle\langle 11|). \quad (1.30)$$

This state is obviously entangled. In fact, all the subsystems are in a completely mixed state.

When considering any of the two qubits (e.g. the first two, any of them can be chosen for symmetry reasons), however, using the formula in (1.28), for this density operator, we get $C(\rho_{12}) = 0$. This means that state (1.30) is a separable state or, in other words, the first two quantum bits are not entangled with each other as a pair.

It means that in the present entangled state there is no qubit-pair entanglement whatsoever. Indeed, after carrying out a measurement on the third quantum bit in the basis $|0\rangle, |1\rangle$, the state of the first two quantum bits will be either $|00\rangle$ or $|11\rangle$ with equal probability. This means that the bipartite state can be constructed as a convex combination of separable pure states.

So the entanglement of the first two quantum bits can be juggled away by achieving measurement on the third one. Due to the symmetry of the state, this holds true of the case of any pair of quantum bits in this state. In the GHZ state (1.29), the state of any quantum bit pair can be separated. The whole system is an entangled state, after all! State (1.29) is not separable. This can be seen, if we choose one of the three quantum bits, its state, according to (1.18), is a maximally mixed state, that is, the chosen quantum bit is maximally entangled with the subsystem of the other two quantum bits.

Hence, the entanglement present in this state is *genuine threepartite*. Interestingly, it can be converted to maximal bipartite entanglement though. Carrying out a properly chosen measurement on one of the

quantum bits, we can make the state of the system of other two quantum bits maximally entangled. Indeed, if the eigenvectors of the measurement are now $\frac{1}{\sqrt{2}}(|0\rangle \pm |1\rangle)$, we get the maximally entangled states $\frac{1}{\sqrt{2}}(|00\rangle \pm |11\rangle)$ with equal probability. Both states are maximally entangled bipartite states. If we are aware of the measurement result, we know which state we have obtained, so we can use it, e.g. for teleportation. In this system, its tripartite entanglement can be completely converted into a bipartite entanglement.

1.2.4 Monogamy of entanglement

Note that a maximally entangled state of two quantum bits is necessarily a pure state. Hence two quantum bits cannot be entangled with any other system. This means that (unlike classical correlations) quantum entanglement has a property which is called *monogamy*: pairwise entanglement of two subsystems limits the entanglement with the other subsystems.

As for a quantitative description of monogamy, we introduce another quantity which we will use in our work. This is the *tangle* denoted by τ , which is the linear entropy in Eq. (1.21) of a given subsystem, which, for qubits can also be expressed as

$$\tau_k = 4\det\rho(k).$$

This is the so-called one-tangle, characterizing the entanglement between the given qubit and the rest of the total system which is in a pure state. In case we have two qubits in a pure state, the tangle relating to one of them equals the square of the concurrence. Let us consider a system consisting of many qubits and suppose the system is in a pure state. Checking concurrences of the qubit pairs in the system, we get that Coffmann-Kundu-Wootters (CKW) inequalities [2] are satisfied:

$$\tau_k \geq \sum_{l \neq k} C_{k,l}^2 \quad (1.31)$$

This formula can be interpreted in the following way: the entanglement measured in tangle between the k -th qubit and the rest of the total system gives an upper bound for the concurrence calculated between the k -th qubit and another arbitrary qubit in the system. If these inequalities are saturated, the bipartite entanglement is maximal.

The CKW inequalities had been originally formulated as a conjecture, but they were later proven. Their saturation reflects that the bipartite entanglement is in a way maximal in the system.

1.3 Quantum cloning

First of all, we have to make the meaning of word *quantum cloning* clear. Suppose we would like to build a machine which is able to create a perfect replica of an arbitrary system being in an unknown quantum state. A tool like that seems to be necessary for certain information processing tasks. Error correction, for instance, could be done using procedures making use of several perfect copies of the original system carrying the information. Such a creation of one or more exact replicas of physical systems in arbitrary (unknown) quantum states is termed as quantum cloning. The reason for the name, as we shall see, is that the “cloned” system cannot be in fact distinguished from the original one.

It is natural to ask if the laws of quantum mechanics allow us to build such a machine. To put it formally, we consider e.g. a quantum bit in the state. $|\Psi\rangle = \alpha|0\rangle + \beta|1\rangle$. In addition we need an ancillary system which will be the replica. Its initial state can be arbitrary, say $|0\rangle$ w.l.o.g. The desired operation is then

$$|\Psi\rangle|0\rangle \rightarrow |\Psi\rangle|\Psi\rangle. \quad (1.32)$$

Let us first assume that an arbitrary state, say $|\Psi_1\rangle$ can be simply cloned by a unitary operator U :

$$U|\Psi_1\rangle|0\rangle = |\Psi_1\rangle|\Psi_1\rangle. \quad (1.33)$$

If our machine works as we expected, we can continue cloning with another state $|\Psi_2\rangle$. The state of the target qubit is the same before. In this case we get the following states:

$$U|\Psi_2\rangle|0\rangle = |\Psi_2\rangle|\Psi_2\rangle. \quad (1.34)$$

Due to the unitarity, inner product of the left sides of equations 1.33 and 1.34 has to equal the inner product between the right sides of these equations. Hence we obtain the equation below:

$$\langle 0|\langle\Psi_1|U^\dagger U|\Psi_2\rangle|0\rangle = \langle\Psi_1|\Psi_2\rangle^2.$$

After simplifying, we get the following form:

$$\langle \Psi_1 | \Psi_2 \rangle = \langle \Psi_1 | \Psi_2 \rangle^2. \quad (1.35)$$

From equation 1.35, it directly follows that

$$\langle \Psi_1 | \Psi_2 \rangle = \begin{cases} 0 \\ 1 \end{cases}. \quad (1.36)$$

As we can see in Eq. (1.36), our basic assumption (namely: quantum cloning is a unitary map) leads us results which can be true if and only if we have a total knowledge of the states to be cloned. Obviously, if we knew everything about these states, we would be able to create them without using any device to clone.

More generally it can be shown that the cloning map in Eq. (1.32) is not completely positive, so it is not physical. And this holds not only for quantum bits, but also for any kind of quantum systems. This is the *no cloning theorem* of quantum mechanics first pointed out by Żurek [3].

While thus far we have argued that cloning would be a useful operation in information processing, it is easy to see that the fact of its impossibility has also positive implications from practical point of view. For instance it is a basic ingredient of quantum cryptography. If quantum cloning – in the sense of creating perfect replicas of an unknown state – were a possible map, this protocol would be breakable, because an eavesdropper, after the cloning of the quantum system transmitted between the parties, could achieve measurements on the clones of the qubits sent by Alice to Bob and the quantum key distribution were not secure anymore.

Albeit quantum cloning is an impossible quantum map [3], it is still possible to create imperfect replicas of a quantum state with optimal fidelity [4]. This protocol, originally introduced by Bužek and Hillery [5], is called quantum cloning. It is also possible to perform asymmetric quantum cloning: the fidelity of the copies might not be equal [6, 7]. Quantum cloning has been studied very extensively in the literature, and it has many variants. See Ref. [8] for a review.

In this study we are interested in asymmetric universal cloning transformations for individual quantum bits. A quantum circuit was designed by Bužek et al. for this purpose [9], which was later generalized

to arbitrary dimensional quantum systems [10]. We shall call this circuit UCQC (universal covariant quantum cloner) in what follows. It has a special feature of being quantum controlled, that is, the fidelity ratio of the two clones is controlled by the initial quantum state of two ancillary quantum bits (one of which will carry the clone after the process). This idea turned out to be related to the concept of programmable quantum networks or quantum processors [11]. These are fixed quantum networks which are capable of performing operations on quantum systems in a way that the operation itself is encoded into the initial quantum state of ancillae. It was found that the very circuit for universal quantum cloning is in fact a probabilistic universal quantum processor [12].

In this dissertation we consider UCQC-s as entanglement manipulation devices. In the context of cloning, one may ask several questions. One may consider the cloning of an entangled quantum state as a whole, in order to obtain similar entangled pairs. For two qubits this has been analyzed in detail by several authors [13, 14, 15]. In particular, Bužek et al. [16] compare the fidelity of cloning of an entangled pair by global and local operations.

Another approach might be the broadcasting of entanglement, proposed by Bužek et al. [16]. In this case two parties share an entangled pair and use cloners locally to obtain two partially entangled pairs. This protocol attracted a relevant attention in the literature, too. Topics such as state-dependent broadcasting [17], broadcasting of multipartite entangled states: W-states [17, 18], GHZ-states [19], and linear optical realizations [20] were discussed in detail.

1.4 Interaction-free measurement

Interaction-free measurement (IFM) is an intriguing paradox of quantum mechanics stemming from wave-particle duality. Let us recall the IFM setup and also its explanation of Geszti in Ref. [30], which motivated a part of our results.

The scenario is depicted in Fig. 1.1 In a Mach-Zehnder interferometer, a destructive interference is observed at the detector D in the absence of the absorber, optionally placeable in either of the arms. If the absorber resides in one of the paths, then the detector, which is idle otherwise, will fire. This

is strange since if the absorber had absorbed the particle, there would have been nothing to make the detector fire. Hence, there is a possibility of detecting the presence of the absorber without absorption or, in other words, without interaction. This phenomenon is called interaction-free measurement.

This effect can be viewed as the consequence of the optical theorem of quantum scattering theory: the unitary nature of quantum mechanics does not allow the absorption to be the only effect of an object. The incoming wave should be extinguished by emitting a forward-scattered wave. In this case, the forward-scattered wave can be obtained as a difference between the outgoing wave with an absorber and the outgoing wave with no absorber. To clarify this calculation method of forward-scattered wave, below, we follow the derivation of Tamás Geszti, step by step, in our notation:

As we can see in Fig. 1.1, the Mach-Zehnder interferometer makes possible for a photon to be in either mode d or c , correspondingly the paths towards detectors D or C . Both beam splitters induce transitions between modes d and c . While the probability amplitude of transmission equals $\frac{1}{\sqrt{2}}$, the amplitude of transition equals $\frac{i}{\sqrt{2}}$. As it can be seen from these values, transition happens in half the cases and transmission can be observed in the other half of the cases. For the sake of simplicity, we consider merely two states of the absorber: ground state g and excited state e .

A number of photons can fill the modes d and c . We have to describe three states of this system as its eigenstates. One of these is that the photon is in mode d while the absorber is in its ground state. The other state can be observed, when the photon is in mode c and the absorber is in its ground state. The last one can be detected, if there is no photon in either of the modes but the absorber in its excited state. Hence, the state of the system will be described by a column vector consisting of three representatives. The basis of this state vector can be seen below:

$$|1_d 0_c g\rangle = \begin{pmatrix} 1 \\ 0 \\ 0 \end{pmatrix}, \quad |0_d 1_c g\rangle = \begin{pmatrix} 0 \\ 1 \\ 0 \end{pmatrix}, \quad |0_d 0_c e\rangle = \begin{pmatrix} 0 \\ 0 \\ 1 \end{pmatrix}. \quad (1.37)$$

As it can be seen below, unitary matrices represent the beam splitter and the absorber on this basis:

$$\mathbf{U}_{BS} = \begin{pmatrix} \frac{1}{\sqrt{2}} & \frac{i}{\sqrt{2}} & 0 \\ \frac{i}{\sqrt{2}} & \frac{1}{\sqrt{2}} & 0 \\ 0 & 0 & 1 \end{pmatrix}, \quad \mathbf{U}_{AB} = \begin{pmatrix} 1 & 0 & 0 \\ 0 & 0 & -1 \\ 0 & 1 & 0 \end{pmatrix} \quad (1.38)$$

In this study we work with ideal detectors that covers the members of the basis described above. Carrying out a quantum measurement in this basis, we force the system to choose randomly one of the states that are mutually excluded by each other. These possibilities are the following ones: detecting a photon on mode d (detector D), detecting a photon on mode c (detector C), detecting the absorber in its excited state.

Let us consider the standard treatment of the setup that can be seen in Fig. 1.1 The sequence of the unitary evolution can be drawn in the following way:

$$\begin{pmatrix} 1 \\ 0 \\ 0 \end{pmatrix} \rightarrow \begin{pmatrix} \frac{1}{\sqrt{2}} \\ \frac{i}{\sqrt{2}} \\ 0 \end{pmatrix} \Rightarrow \begin{pmatrix} \frac{1}{\sqrt{2}} \\ 0 \\ \frac{i}{\sqrt{2}} \end{pmatrix} \rightarrow \begin{pmatrix} \frac{1}{2} \\ \frac{i}{2} \\ \frac{i}{\sqrt{2}} \end{pmatrix} \quad (1.39)$$

In the expression above, arrows on right and left stand for the effects of the two beam splitters and the medial one corresponds to the absorber. Now we begin to use the scattering theory to analyze the effect of the absorber. Changes which are caused by the absorber can be found by defining a reference sequence of unitary events without any absorber. In this case \mathbf{U}_{AB} is replaced by unity:

$$\begin{pmatrix} 1 \\ 0 \\ 0 \end{pmatrix} \rightarrow \begin{pmatrix} \frac{1}{\sqrt{2}} \\ \frac{i}{\sqrt{2}} \\ 0 \end{pmatrix} \Rightarrow \begin{pmatrix} \frac{1}{\sqrt{2}} \\ \frac{i}{\sqrt{2}} \\ 0 \end{pmatrix} \rightarrow \begin{pmatrix} 0 \\ i \\ 0 \end{pmatrix}. \quad (1.40)$$

On mode d , we get a full destructive interference. Subtracting Eq. (1.40) from Eq. (1.39) results the "scattering amplitude"

$$\begin{pmatrix} 0 \\ 0 \\ 0 \end{pmatrix} \rightarrow \begin{pmatrix} 0 \\ 0 \\ 0 \end{pmatrix} \Rightarrow \begin{pmatrix} 0 \\ -\frac{i}{\sqrt{2}} \\ \frac{i}{\sqrt{2}} \end{pmatrix} \rightarrow \begin{pmatrix} \frac{1}{2} \\ -\frac{i}{2} \\ \frac{i}{\sqrt{2}} \end{pmatrix}. \quad (1.41)$$

This forward-scattered wave gets to the detector, making the interaction-free measurement possible.

1.5 Hardy's paradox

The Hardy paradox [27] is one of the consequences of quantum entanglement: it is a statistical phenomenon which cannot be explained in the realm of *local realism*. It is a concept whose physical and philosophical implications are extensive and far deeper to be even summarized in detail in the present work. Hence we employ the Hardy paradox here not only as the subject of our actual study but also as an illustrational example of the violation of local realism.

The interferometric setup for Hardy's paradox is depicted in Fig. 1.2; we use the notation introduced there in what follows. It consists of two Mach-Zehnder interferometers. An electron impinges on one of them and a positron on the other. There is a point P where they can meet and annihilation may take place.

Hardy's gedanken experiment aims at the testing of local realism without inequalities. The presence or absence of the beam splitters $BS2_{\pm}$ plays the role of the *local setting*, which is a key element also in the case of Bell-type inequalities. Local realism would require that the measurement statistics of, e.g., the electron should be independent of the choice of whether $BS2_{+}$ is in its place or not. As it is clear from the calculations in Section 3.1, if none of the beam splitters is in its place, detectors C_{+} and C_{-} cannot fire in coincidence. On the other hand, local realism would require that the detection probabilities of the positron (electron) should not depend on the presence or absence of the beam splitter for the electron (positron), respectively. From this assumption and the probabilities implied by the calculations in Section 3.1, one can deduce, after a reasoning given in Ref. [27] (not repeated here), that in $\frac{1}{16}$ th of the cases, the independence assumption implied by local realism leads

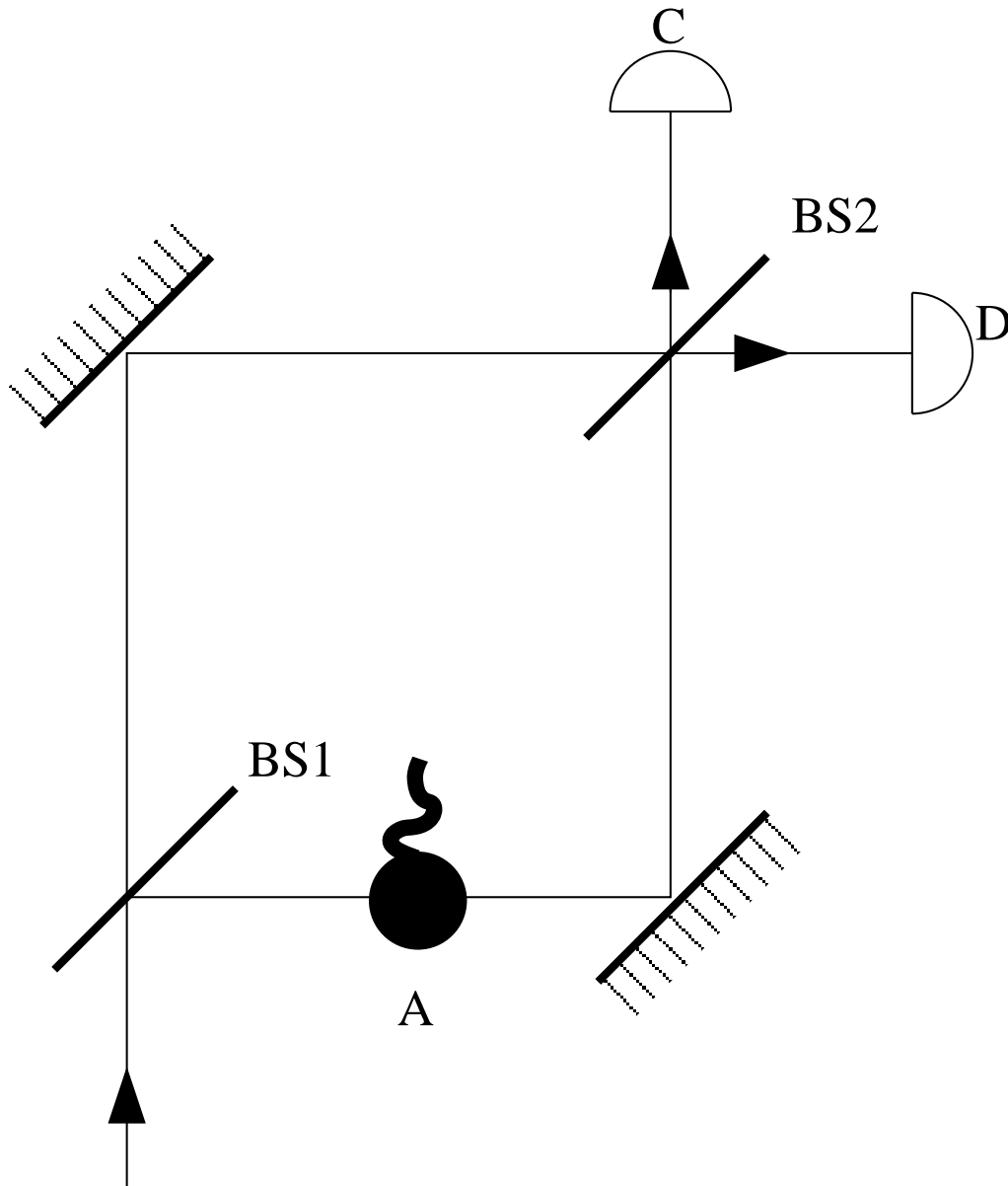


Figure 1.1: The interferometric setup for interaction-free measurement. In the absence of absorber A (say, a bomb (as Elitzur and Vaidman suggested in Ref. [34])), detector D is always idle. If A is there, there is a finite probability that D fires, thus the interfering particle is not absorbed. (Thus the bomb is detected without exploding.)

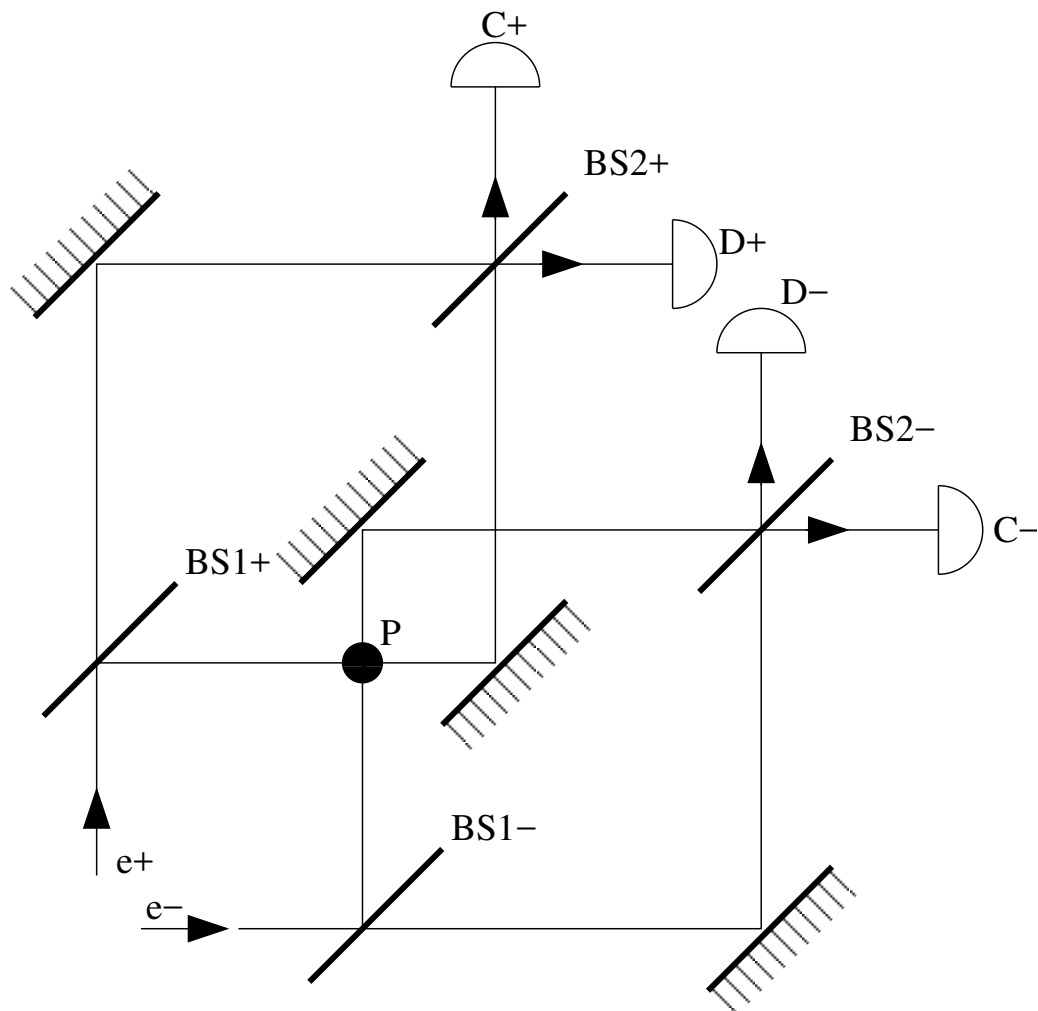


Figure 1.2: The interferometric setup of Hardy's paradox. The electron and the positron may meet at point P only. The beam splitters $BS2_{\pm}$ are optionally replaceable; if they are replaced, the particles reach the respective detector directly. The symbols $c+$, $d+$, $c-$, $d-$ denote the paths in the interferometer to guide the reader's eye. The plus and minus signs in this path notation refer to the type of particle, while the letter corresponds to the detector at the direct (not reflected) end of the path.

to coincident detection at detectors $C+$ and $C-$ for the same situation, which is in contradiction with quantum mechanics.

Having outlined the scientific context and defined the notation, let us now turn to the description of our results.

Chapter 2

Optimal universal asymmetric covariant quantum cloning circuits for qubit entanglement manipulation

In this chapter, we consider the entanglement manipulation capabilities of the universal covariant quantum cloner or quantum processor circuit for quantum bits. We investigate its use for cloning a member of a bipartite or a genuine tripartite entangled state of quantum bits. We find that for bipartite pure entangled states a nontrivial behavior of concurrence appears, while for GHZ entangled states a possibility of the partial extraction of bipartite entanglement can be achieved.

Consider an entangled pair. It is always interesting to ask what happens to the entanglement if any of the members of the pair is subjected to some quantum information processing protocol. In the case of quantum teleportation, for instance, rather strikingly the teleported qubit inherits the entanglement of the original qubit with its pair. It is rather natural to ask what happens in the case of a universal quantum cloner. The answer for qubit pairs is partly given by Bandyopadhyay and Kar [21]. They show that if a member (or both members) of a maximally entangled qubit pair is subjected to an optimal universal quantum cloning operation, the resulting state is a Werner state. It is likely, however, that a cloning transformation is realized by some quantum circuit, which uses ancillae for carrying out

the operation. It is obviously interesting how the entanglement between the different quantum bits of such a scenario (including also ancillae) behaves. In this chapter we consider the UCQC as a circuit, not only the cloning operation itself. We calculate entanglement as measured by concurrence (see Section 1.2). It turns out that the ancillae play a very specific role and the behavior of concurrence shows a rather interesting pattern. The recent optical realization of certain programmable quantum gate arrays [22] also contributes to the relevance of this question.

Another similar question might be the partial extraction of bipartite entanglement from a GHZ-type tripartite resource. It is known that if three qubits are in a GHZ state [23], then a measurement on either of the three qubits in the $|\pm\rangle$ basis (eigenbasis of the σ_x Pauli-operator) projects the state of the remaining two qubits into a maximally entangled state. We show that if the given particle is cloned in advance, it is possible to create bipartite entanglement by measuring the clone, while there still remains some purely tripartite entangled resource in the state of the three parties. This is indicated by the possibility of entangling a different pair of qubits by a next measurement. The nature of the entanglement in the multipartite system can be also analyzed with the aid of the Coffman-Kundu-Wootters inequalities [2] (see Section 1.2), which quantify the monogamy of entanglement. We shall present such an analysis, too.

This chapter is organized as follows: in Section 2.1 we analyze the behavior of bipartite entanglement in the case when UCQC is applied to clone a member of a maximally entangled pair. In Section 2.2 we consider the application of UCQC for the partial extraction of bipartite entanglement from a Greenberger-Horne-Zeilinger state. In Section 2.3 the results are summarized and conclusions are drawn.

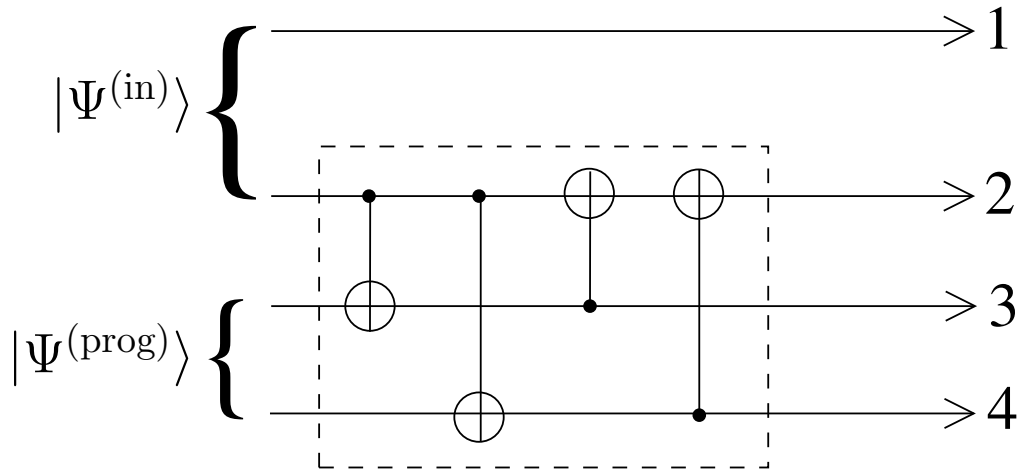


Figure 2.1: The setup for bipartite entangled states. The dashed box contains the universal covariant cloning circuit, composed of four controlled-NOT gates.

2.1 Bipartite pure states

The considered setup is depicted in Fig. 2.1. The quantum circuit in the dashed box is the universal quantum cloner [10]. Its first input port (which is port 2 in our current notation) receives the state to be cloned, while on the second two ports there impinges a so-called program state:

$$|\Psi_{34}^{(\text{prog})}\rangle = \mathcal{N}(\alpha(|0\rangle(|0\rangle + |1\rangle)) + \beta(|00\rangle + |11\rangle)), \quad (2.1)$$

where $\mathcal{N} = 1/\sqrt{2(\alpha + \beta^2)}$ is a normalization constant, α is a real parameter and $\beta = 1 - \alpha$. (In Ref. [9] there is an additional circuit introduced to prepare the program state of Eq. (2.1), as a first step of cloning, which we have omitted here, as it does not have a role in the cloning process itself.)

Were a single-qubit state ϱ impinging on port 2, the output states would be:

$$\begin{aligned} \varrho_2 &= \frac{\beta}{\alpha + \beta^2} \varrho + \frac{\alpha^2}{2(\alpha + \beta^2)} \hat{1}, \\ \varrho_3 &= \frac{\alpha}{\beta + \alpha^2} \varrho + \frac{\beta^2}{2(\beta + \alpha^2)} \hat{1}, \\ \varrho_4 &= \frac{\alpha\beta}{\beta^2 + \alpha} \varrho^T + \frac{\alpha^2 + \beta^2}{2(\alpha + \beta^2)} \hat{1}. \end{aligned} \quad (2.2)$$

The clones reside in ports 2 and 3, the original qubit and the first ancilla, whereas in the port 4 there is an ancilla, the state of which is a mixture of the state described by the mixture of the transpose of

the density operator of the original state and the identity operator. The fidelity of the clones depends on the value of α : for $\alpha = 0$ there is no cloning, whereas for $\alpha = 1$ the state of the original qubit is fully transferred to the clone, leaving the original qubit in a completely mixed state. For other values of alpha there are optimal clones generated. Note the symmetry of the formulae in α and β .

In the terminology of cloning this setup realizes an optimal universal asymmetric cloner. The term asymmetric expresses that the two clones are not identical, their fidelity with respect to the original state is different, but controlled by the parameter α . Setting $\alpha = \frac{1}{2}$, we obtain the symmetric case. The cloning is universal in the sense that the realized cloning transformation itself does not depend on the input state. Optimality in this context means that the second clone is obtained with maximal fidelity for a given fidelity of the first one.

Let us return to the description of the whole scenario in argument, depicted in Fig. 2.1. The qubits 1 and 2 carry the initial bipartite input state. Qubit 2 is subject to cloning, while qubit 1, the first part of the pair is not manipulated. We are interested in the entanglement relations between the different pairs of qubits in the resulting state. As for the measure of bipartite entanglement for qubits, we apply concurrence according to the Wootters formula as we saw in Eq. (1.28).

As an input state we consider a state in either of the following four forms:

$$\begin{aligned}
 |\Phi_{12}^{(\text{in})}\rangle &= \sqrt{C_0}|00\rangle \pm \sqrt{C_1}|11\rangle, \\
 &\text{or} \\
 |\Psi_{12}^{(\text{in})}\rangle &= \sqrt{C_0}|01\rangle \pm \sqrt{C_1}|10\rangle, \\
 C_0 + C_1 &= 1.
 \end{aligned} \tag{2.3}$$

As for the nonzero concurrences between the various pairs of qubits, we obtain the behavior in Fig. 2.2, regardless of the choice from the above states. The output states, however, depend on this actual choice, we shall comment on this later.

In the figure one can observe that the entanglement between qubits 1 (the one not manipulated) and qubit 2 (the original qubit) behaves in the similar way as that between qubit 1 and 3 (the one not manipulated and the clone). For $\alpha = 0$ (no cloning), qubits 1 and 2 are entangled as they were

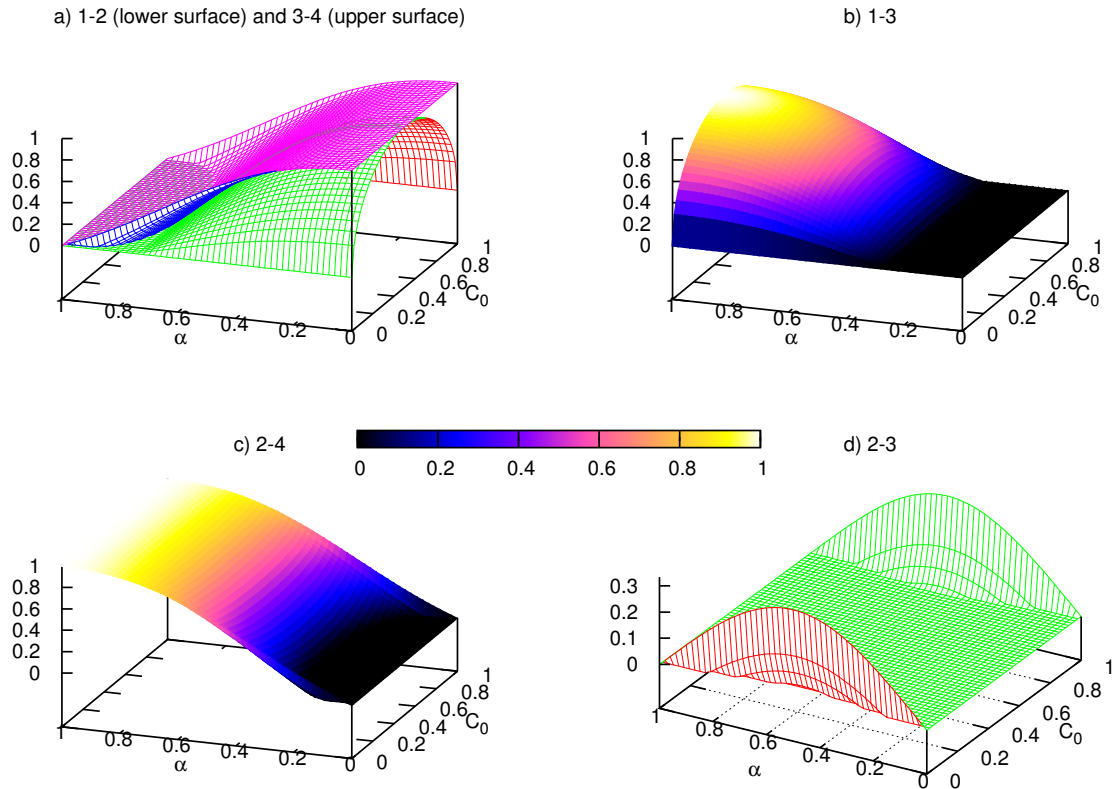


Figure 2.2: (color online) The concurrence between the various pairs of qubits at the output of the setup in Fig. 2.1. The input state is either of the four in Eq. (2.3), the same figure is obtained for each choice, though the states themselves differ. The “program” state is the one in Eq.(2.1). The concurrence between qubits 1 and 4 is zero. The plotted quantities are dimensionless.

originally, while for $\alpha = 1$, complete cloning, the entanglement is transferred to qubits 1 and 3, the clone plays the role of the former original qubit completely. The surfaces representing the concurrence for the pairs 1-2 and 1-3 are symmetric in the cloning parameter α , that is, they can be obtained from each other by the $\alpha \rightarrow 1 - \alpha$ substitution. The dependence of these entanglements from α is monotonous but not continuous: for small values there is a region where the entanglement is zero, and it appears suddenly and non continuously. The dependence of these concurrences on the initial entanglement in the state C_0 is monotonous and continuous.

It is also interesting to observe that a similar non-symmetric behavior appears in the concurrence of qubits 3-4 and 2-4. The program state of Eq. (2.1), in which the qubits 3-4 are prepared initially, is maximally entangled for $\alpha = 0$, the case of no cloning, and its entanglement decreases with the increase of the cloning parameter α . Accordingly, the entanglement of qubits 3-4 decreases with α also after the cloning operation, while the complementary behavior (in the sense of $\alpha \rightarrow 1 - \alpha$ substitution) appears between qubits 2 and 4 (the cloned part of the input state and the ancilla of the cloner). Note that the entanglement of qubits 3 and 4 is not equal to their entanglement *before* the cloning operation: the concurrence of the partially entangled program state in Eq. (2.1) is a monotonous and continuous function of α , and its values are not equal to the concurrences after the cloning operation. Moreover, the concurrence of qubits 3 and 4 after the cloning also depends slightly on that of the input state of qubits 1 and 2, in Eq. (2.3).

As for the remaining pairs, qubits 1 and 4 (the qubit not manipulated and the ancilla) will not be entangled, while between qubits 2 and 3 (the second input state and its clone), as a nontrivial effect, there is a small amount of entanglement appearing only in the case the input state (of qubits 1-2) is only slightly entangled.

A special case arises if the input state of qubits 1 and 2 is maximally entangled. This is the case of $C_0 = 1/2$ in Fig 2.2. The concurrence between qubits 1-2 and 3-4 (two originals, two program qubits of the cloner) is equal to each other. The complementary pairs, qubits 1-3 (not manipulated-clone) and 2-4 (clone-ancilla) have also equal concurrences. The dependence of these concurrences on α is depicted in Fig. 2.3. The behavior of these curves is due to the fact that the universal cloning

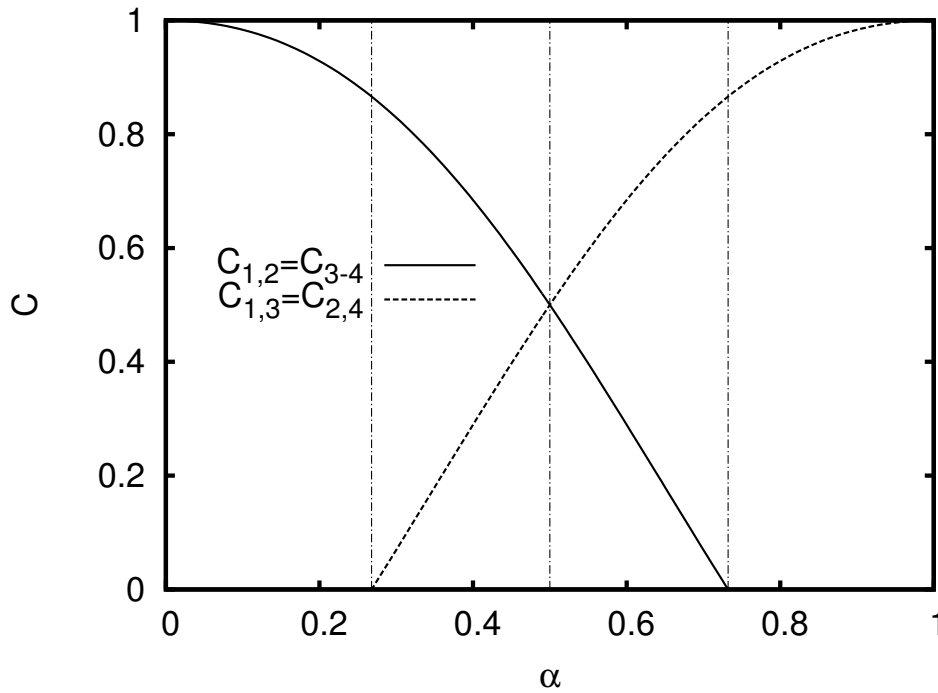


Figure 2.3: A slice of Figs. 2.2 a-c) for $C_0 = 1/2$, that is, for any of the maximally entangled Bell-states as input. The plotted quantities are dimensionless.

transformation produces Werner states. Indeed, if the input state in Eq. (2.3) is the maximally entangled $|\Phi^{(+)}\rangle$ Bell-state, where the states of qubit-pairs 1-2, 1-3, 2-4, 3-4 are Werner-states of the form

$$\rho^{(\text{Werner})} = \gamma |\Phi^{(+)}\rangle\langle\Phi^{(+)}| + \frac{1-\gamma}{4} \hat{1}, \quad (2.4)$$

where $\hat{1}$ stands for the identity operator of the two-qubit space. The value of the parameter γ is

$$\gamma_{12} = \gamma_{34} = \frac{\alpha}{\alpha + \beta^2} \quad (2.5)$$

for pairs 1-2 and 3-4, while it is

$$\gamma_{13} = \gamma_{24} = \frac{\beta}{\alpha + \beta^2}. \quad (2.6)$$

Note that the denominator on the right-hand-side of the above formulae comes directly from the normalization constant of the program state in Eq. (2.1) (i.e. the scaling of parameters in Eqs. (2.5) and (2.6) is merely a consequence of our particular choice of parameters). In the case we choose a different one from the states in Eq. (2.3), we obtain local unitary transforms of the Werner state in

Eq. (2.5). The message of the consideration for cloning an element of a maximally entangled pair is not the fact that Werner states are obtained in qubits 1-2 and 1-3, since it was known from the literature [21]. What is nontrivial here that in the UCQC circuit this behavior is repeated between the ancilla (qubit 4), and qubits 2 and 3, and this holds only in the case of the cloning of a member of a maximally entangled state. Finally let us note that the behavior of qubits 2, 3, and 4 cannot depend on the properties of qubit 1 since it is a remote system from the UCQC's point of view. It is the reduced density operator of qubit 2 which can influence their behavior. We have found that only for a maximally entangled pair, a concurrence characterizing a nonlocal property is equal to another concurrence which is a local property of the cloner.

2.2 The GHZ state

In this section we consider the case in which a member of a Greenberger-Horne-Zeilinger (GHZ) state is cloned. This tripartite state, of the form

$$|\Psi^{(GHZ)}\rangle = \frac{1}{\sqrt{2}}(|000\rangle + |111\rangle) \quad (2.7)$$

is known to be genuinely tripartite entangled. That is, all the pairwise entanglements (as measured by concurrence) are zero, however, all of the three qubits are in a maximally entangled state. When any of the qubits is subject to a von Neumann measurement in the basis

$$|\pm\rangle = \frac{1}{\sqrt{2}}(|0\rangle \pm |1\rangle), \quad (2.8)$$

the other two qubits will be in either of the maximally entangled Bell-states

$$|\Phi^\pm\rangle = \frac{1}{\sqrt{2}}(|00\rangle \pm |11\rangle), \quad (2.9)$$

depending on the measurement result. The probability of the measurement results are equal. In this way the tripartite entangled resource in the GHZ state can be converted into maximal bipartite entanglement.

The scenario we consider for GHZ states is depicted in Fig. 2.4. Qubits 1-3 carry the input state which

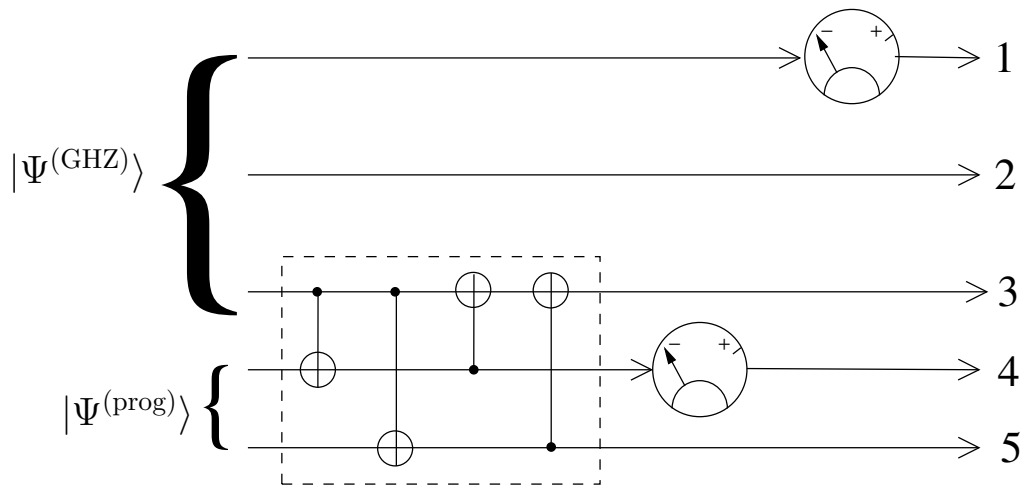


Figure 2.4: The setup for the tripartite GHZ state. Qubits 1-3 hold the GHZ state initially. The dashed box contains the universal covariant cloning circuit, composed of four controlled-NOT gates. The “meters” measure in the $|\pm\rangle$ basis. First the clone (qubit 4), then a member of the original GHZ state (qubit 1) is measured. The horizontal position from the left to the right side thus represents the order of operations in time.

is a GHZ state in Eq. (2.7). Qubit 3 enters the UCQC’s first port. The program ports of the UCQC are qubits 4 and 5, considered again to be in the program state in Eq. (2.1).

Directly after the operation of the cloner all pairwise concurrences are zero, except for the one between qubits 3-5 and 4-5. Their value is represented by curves “A” and “B” in Fig. 2.5. This fact is easily explained by the following reasoning. From the point of view of the UCQC circuit, qubits 1 and 2 are remote ones, thus they cannot influence the local properties of qubits 3, 4 and 5. All we “see” at the locus of the UCQC is that qubit 3 is in a maximally mixed state, as it is a member of the maximally entangled tripartite GHZ state of Eq (2.7). But the same situation would arise if qubit 3 were maximally entangled in a bipartite sense with one additional qubit, as we have considered in the previous Section. Thus the behavior of concurrences between the pairs ancilla-original and ancilla-clone are the very same as in the case of cloning a member of a bipartite maximally entangled state (or a member of any kind of multipartite entangled state which is itself in a completely mixed state for this reason): Werner states are obtained.

Projective measurement on the clone. Motivated by the relation of the projective measurements of the members of a GHZ state on the $|\pm\rangle$ basis, one may now consider a measurement of this kind on the clone, that is, on qubit 4. This measurement will not alter the bipartite entanglement between qubits 3-5, and that between 4-5 will disappear due to the measurement. However, there will be an even larger entanglement appearing between qubits 1 and 2, this is curve “C” in Fig. 2.5. Both measurement outcomes will have equal probability and also the entanglement behavior is the same for both cases. In case of full cloning ($\alpha = 1$), we obtain a pure EPR pair as expected. (We remark here that if we were to measure on the original qubit (qubit 3) instead of its clone, we would obtain the counter propagating curve of the same shape, curve “D” in Fig. 2.5, as one would expect. The role of the original and the clone is symmetric. Entanglement of 4-5 will not alter, while that of 3-5 will disappear in this case.) This is a partial conversion of the resource available as genuine tripartite entanglement into bipartite entanglement.

Measurement on the qubit 1. In order to further justify this statement let us consider a second measurement, now on qubit 1. Again, the results will be uniformly distributed and the entanglement itself will not depend on the measurement result. The entanglement between qubits 3 and 5 will be untouched, and that between qubits 1 and 2 will be destroyed by the measurement of course. Meanwhile we obtain nonzero entanglement between pairs 2-3 and 2-5, these are the curves “D” and “E” in Fig. 2.5, respectively. Indeed, if the extraction of the tripartite entanglement was not full (i.e. $\alpha \neq 1$), one can still obtain bipartite entanglement by measuring another qubit this time. Curves “C” and “D”, describing the entanglement between 1-2 after the first measurement, and that between 2-3 after the second measurement, respectively, are counter propagating, reflecting the interplay between the two extractions. As a side effect, there is a small amount of entanglement which appears between qubits 2-5 after the second measurement, this is curve “E” in Fig. 2.5.

The use of the partial extraction of the entanglement is the following. Consider that qubit 1 is at Alice, qubit 2 at Bob, while the rest of the qubits is at Charlie. Initially they share a tripartite GHZ resource. Charlie wants to enable Alice and Bob to use a bipartite maximally entangled channel. He might perform the projective measurement on the clone he has, however, in this case his qubit 3 gets

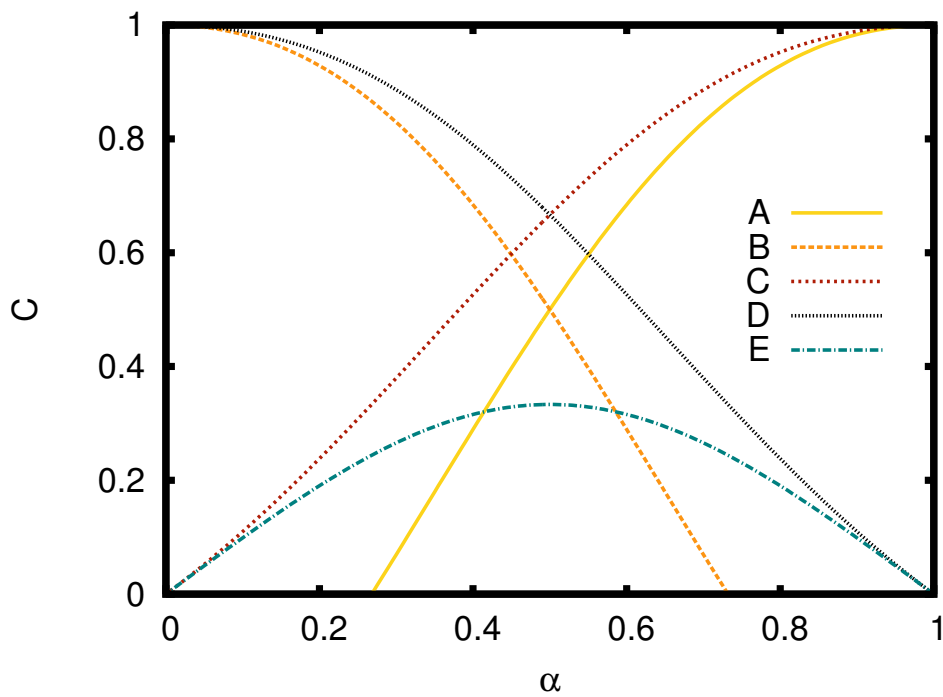


Figure 2.5: (color online) Pairwise concurrences in the GHZ-cloning scenario. A: qubits 3-5 after the cloner and also after each measurement, B: qubits 4-5 after the operation of the cloner, C: qubits 1-2 after the first measurement, D: qubits 2-3 after the second measurement, E: qubits 2-5 after the second measurement. The plotted quantities are dimensionless.

disentangled from the rest of the parties. However, if he performs cloning and measures the clone, Alice and Bob still obtains a partially entangled bipartite resource. However, Alice can decide that instead of using a bipartite channel with Bob, she wants to create a channel between Bob and Charlie. All she has to do is to perform a proper measurement on her qubit and communicate the result: Bob and Charlie shall possess a partially entangled bipartite resource. This would not be possible without the cloning. The same could be done of course by Bob, to enable the bipartite resource between Alice and Charlie.

In order to obtain a deeper insight into the behavior of bipartite entanglement in this multipartite system, it is worth examining the Coffman-Kundu-Wootters inequalities. As we mentioned in Section 1.2, if inequalities in Eq. (1.31) are saturated, the bipartite entanglement is maximal.

To quantify the saturation we evaluate

$$s = \tau_k - \sum_{l \neq k} C_{k,l}^2, \quad (2.10)$$

which is zero if the inequalities are saturated. After the first measurement we obtain nonzero values except for the fourth qubit (apart from the case of $\alpha = 1$). The behavior is depicted in Fig. 2.6. The fact that the CKW inequalities are not saturated also suggests the presence of additional multipartite entanglement in the system. After the second measurement, on the other hand, we find that all the CKW inequalities are saturated: the system is in a sense maximally bipartite entangled.

2.3 Conclusion

We have shown that when using a universal covariant quantum cloning circuit to clone a member of an entangled pair of qubits, a very specific behavior of the entanglement of the qubits appears. The main feature is that behavior of the entanglement between the not cloned part of the pair and the cloned one is repeated in the entanglement of certain ancillae, and so is that of the not cloned qubit and the clone, provided that the original qubit pair was maximally entangled initially. We have described the behavior of the entanglement in detail.

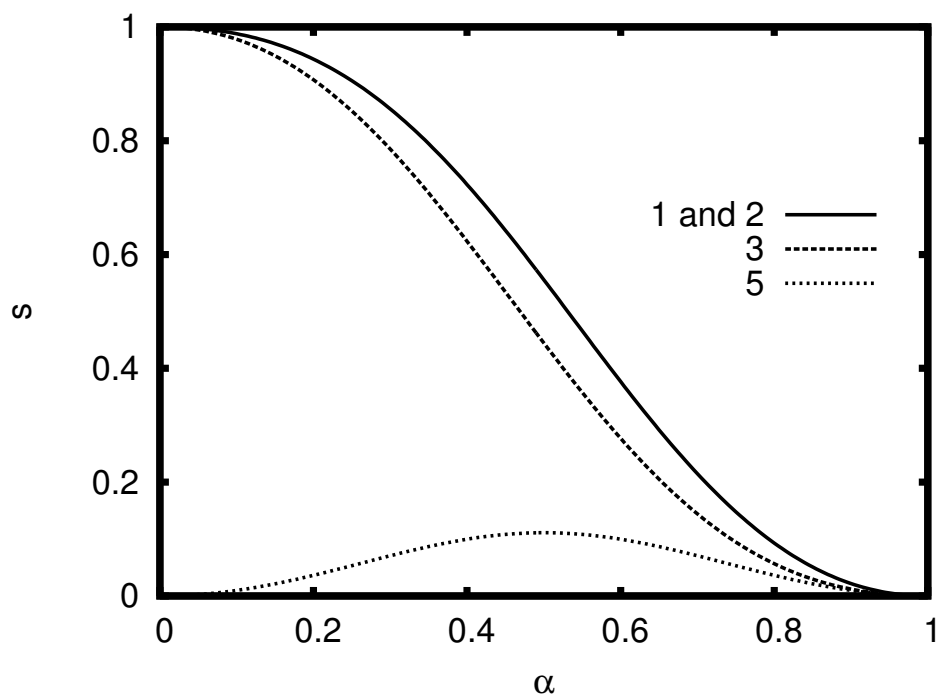


Figure 2.6: The quantity in Eq. (2.10), which is zero if the CKW inequalities are saturated, for each qubit after the first measurement in our GHZ-cloning scenario. For qubit 4 the quantity is zero. The plotted quantities are dimensionless.

We have also investigated the cloning of an element of the GHZ state. It appears that the universal quantum cloning circuit facilitates the partial extraction of bipartite entangled resources from a genuine tripartite entangled resource. We provided a detailed analysis of the entanglement behavior, including the relation to Coffman-Kundu-Wootters inequalities.

In conclusion, the universal quantum cloning circuit (or quantum processor) for qubits is found to be useful as an entanglement manipulator as well. It can perform entanglement manipulations which are potentially applicable in quantum information processing.

Chapter 3

Hardy's paradox and the entanglementlike structure of forward-scattered waves

In this chapter we analyze Hardy's paradox, which we have introduced in Section 1.5. Our analysis starts from the observation that the scheme in which the paradox is observed is similar to that of interaction-free measurement. As described in Section 1.4, this latter can be better understood with an approach originating in scattering theory. The idea behind our investigation was whether we employ Geszti's approach to Hardy's scenario.

3.1 The setup

Let us first recapitulate the original calculations of Ref. [27] as they are required to derive our results.

We use the notation of Fig. 1.2. We have four possible arrangements of the beam splitters, which are the following:

1. $BS2+$ and $BS2-$ are removed.
2. $BS2+$ is in place, $BS2-$ is removed.

3. $BS2+$ is removed, $BS2-$ is in place.
4. $BS2+$ and $BS2-$ are in place.

Let us denote the modes of the Mach-Zender interferometers by $P_d, P_c, E_d,$ and E_c , where the letters c and d distinguish the two modes of the interferometer, while P and E describe the positron and the electron, respectively. The beam splitters utilized in the setup are considered to be symmetric, with reflection coefficient $\frac{i}{\sqrt{2}}$ and transmission coefficient $\frac{1}{\sqrt{2}}$. The state of the system of the two interferometers lies in the tensor-product space of three Hilbert spaces, namely, $\mathcal{H}_p, \mathcal{H}_e,$ and \mathcal{H}_γ , where \mathcal{H}_p is the Hilbert space of the positron, \mathcal{H}_e is the Hilbert space of the electron, and \mathcal{H}_γ is the Hilbert space of the electromagnetic-field mode of the γ photon emitted upon annihilation.

Both \mathcal{H}_p and \mathcal{H}_e contain three basis states, which can have nonzero coefficients in this setup. The state $|p_0\rangle, |e_0\rangle$ correspond to the situation in which there is no particle in either arm (c, d) of the respective interferometer. Kets $|p_d\rangle, |e_d\rangle$ denote the basis states that correspond to the situation when the respective particle is in mode d . Finally, the state where the respective particle is in mode c is denoted by $|p_c\rangle, |e_c\rangle$. Since, at most, one photon can be created in the annihilation, \mathcal{H}_γ is spanned by two elements of the bases: the vacuum $|\gamma_0\rangle$ and the single-photon state $|\gamma_1\rangle$. The state of the whole system can be expressed as the linear combination of the following orthogonal product states:

- i. $|p_0\rangle|e_0\rangle|\gamma_1\rangle = |\gamma\rangle$. There is no positron or electron in the arms because they have annihilated each other, and there is a photon emitted.
- ii. $|p_d\rangle|e_d\rangle|\gamma_0\rangle = |p_d e_d\rangle$. Both the positron and the electron are in mode d , and the photon is absent.
- iii. $|p_d\rangle|e_c\rangle|\gamma_0\rangle = |p_d e_c\rangle$. The positron is in mode d , the electron is in mode c , and the photon is absent.
- iv. $|p_c\rangle|e_d\rangle|\gamma_0\rangle = |p_c e_d\rangle$. The positron is in mode c , the electron is in mode d , and the photon is absent.

- v. $|p_c\rangle|e_c\rangle|\gamma_0\rangle = |p_c e_c\rangle$. The positron is in mode c , the electron is in mode c , and the photon is absent.

If we consider the four aforementioned arrangements of the beam splitters, we will find four outgoing states correspondingly (denoted by $|\text{out}1\rangle$, $|\text{out}2\rangle$, $|\text{out}3\rangle$, and $|\text{out}4\rangle$), in accordance with the results in Ref. [27]. In the absence of both beam splitters, the output state reads

$$|\text{out}1\rangle = \frac{1}{2}(-|\gamma\rangle + |p_d e_d\rangle + i|p_d e_c\rangle + i|p_c e_d\rangle), \quad (3.1)$$

while the output states for $BS2+$, $BS2-$, and both, respectively, are

$$|\text{out}2\rangle = -\frac{\sqrt{2}}{4}(-\sqrt{2}|\gamma\rangle + i|p_d e_c\rangle + 2i|p_c e_d\rangle - |p_c e_c\rangle), \quad (3.2)$$

$$|\text{out}3\rangle = -\frac{\sqrt{2}}{4}(-\sqrt{2}|\gamma\rangle + 2i|p_d e_c\rangle + i|p_c e_d\rangle - |p_c e_c\rangle), \quad (3.3)$$

$$|\text{out}4\rangle = \frac{1}{4}(-2|\gamma\rangle - |p_d e_d\rangle + i|p_d e_c\rangle + i|p_c e_d\rangle - 3|p_c e_c\rangle), \quad (3.4)$$

where the incoming state is always $|p_d e_d\rangle$.

3.2 Forward scattering

It is apparent that the setup resembles that of interaction-free measurement to some extent. This suggests that the two phenomena might be related. Indeed, qualitatively it is clear that the two interferometers play the role of a detector for each other, and thus they realize a kind of simultaneous interaction-free measurement. Applying the reasoning in Ref. [30] directly by analyzing the role of point P as a scattering center, one gets the interaction-free measurement based on one of the particles reflecting the presence of the interferometer of the other particle, with a possibility of annihilation at point P . In the case of Hardy's paradox, however, this possibility of annihilation is always present, thus it is not the aim of the experiment to detect the possibility of annihilation. The relevant issue in this case is that the output beam splitters $BS2+$ and $BS2-$ may be removed independently or, in other words, their reflectivity coefficients may be set to zero. The respective paths go directly to the detectors in that case.

Looking at the Hardy situation, however, another possibility appears to be reasonable. Note that here the beam splitters play the role of the optionally replaceable components: the key element of the paradox is to either place or remove the beam splitters locally. We may consider these objects as scattering centers, though with two input and two output modes. There are three possibilities for calculating forward scattering amplitudes. In each case, the reference will be the absence of both beam splitters, but one can decide which of the beam splitters ($BS2+$ and $BS2-$) are in their place. As the beam splitters are local objects, one might expect that the forward-scattered wave generated by either of the beam splitters does not influence that of the other beam splitter. We shall see that this is not the case.

Let us calculate the three forward-scattered waves (denoted by $|fsw+\rangle$, $|fsw-\rangle$, and $|fsw\pm\rangle$) corresponding to the cases when only $BS2+$, only $BS2-$, or both are present, respectively, as follows:

$$|fsw+\rangle = |out2\rangle - |out1\rangle = \frac{\sqrt{2}}{4}[-\sqrt{2}|p_d e_d\rangle + i(1 - \sqrt{2})|p_d e_c\rangle + i(2 - \sqrt{2})|p_c e_d\rangle - |p_c e_c\rangle], \quad (3.5)$$

$$|fsw-\rangle = |out3\rangle - |out1\rangle = \frac{\sqrt{2}}{4}[-\sqrt{2}|p_d e_d\rangle + i(2 - \sqrt{2})|p_d e_c\rangle + i(1 - \sqrt{2})|p_c e_d\rangle - |p_c e_c\rangle], \quad (3.6)$$

$$|fsw\pm\rangle = |out4\rangle - |out1\rangle = -\frac{1}{4}(3|p_d e_d\rangle + i|p_d e_c\rangle + i|p_c e_d\rangle + 3|p_c e_c\rangle). \quad (3.7)$$

It appears that $|fsw+\rangle$ and $|fsw-\rangle$ are symmetric with respect to the amplitudes of $|p_d e_c\rangle$ and $|p_c e_d\rangle$, and it is clear that $|fsw\pm\rangle$ cannot be obtained as a linear combination of $|fsw+\rangle$ and $|fsw-\rangle$. Hence, the forward-scattered waves are not independent; they are, indeed, nonlocal. It is also interesting to note that the photon has no amplitude in the forward-scattered waves. At the level of beam splitters, the possibility of annihilation does not appear in the forward-scattered waves, even though the observed kind of nonlocality is definitely a consequence of the possibility of the annihilation. This can be considered as a manifestation of interaction-free measurement in this case.

Motivated by this nonlocal nature of forward-scattered waves of the beam splitters, one may consider a quantitative measure of quantum correlations in this wave. Even though the forward-scattered wave

does not describe a state of a physical system (it is not even normalized), it plays a definite role in the measurement probabilities. Hence, it is interesting to analyze the extent to which an imaginary physical system, whose state is described by the normalized version of the forward-scattered amplitude, would have an entanglementlike structure, as it reflects the very quantum nature of the correlations.

Let us note that the systems which belong to $BS2+$ and $BS2-$ are effectively two-state systems: in the states $|fsw+\rangle$, $|fsw-\rangle$, and $|fsw\pm\rangle$, there are no amplitudes for which the photon mode is not in the vacuum state. Of course, the complete description of positron and electron states includes their annihilation at point P (see Fig. 1.2), however, the forward-scattered wave has zero probability amplitude for the annihilation. Thus the state represented by the forward-scattered waves resides in a state space spanned by the remaining four basis vectors, which, however, obeys a tensor-product structure of two local bases of two elements each:

$$\{|p_c\rangle, |p_d\rangle\} \text{ and } \{|e_c\rangle, |e_d\rangle\} \quad (3.8)$$

We may consider the system as that of two quantum bits, with one corresponding to the electron and the other to the positron, and the two orthogonal states are represented by the output spatial modes of the beam splitters. (This does not apply for the whole description of the system; it applies to the forward-scattered wave only.) Due to this fact, we can calculate the concurrence for the forward-scattered waves after the normalization of their states using the Wootters formula [1] (presented in Eq. (1.28)) in order to quantify entanglement.

Let us denote the concurrence for the case when $BS2+$ is in place and $BS2-$ is removed by C_+ , and the other two concurrences by C_- and C_{\pm} . After a straightforward calculation, we find

$$\begin{aligned} C_+ = C_- &= \frac{2}{3} \\ C_{\pm} &= 1. \end{aligned} \quad (3.9)$$

These results unambiguously indicate that the normalized forward-scattered wave has an entanglementlike structure: if it were to describe a physical system, that would be an entangled one. Moreover, in the case when both beam splitters are present, its entanglement as measured by concurrence is maximal. It is also interesting to note that the value of concurrence of $\frac{2}{3}$ appearing in the two other

cases is rather special, as it is pointed out in Ref. [31]: it is the concurrence of assistance [32] of a density matrix of rank 3 in the two-qubit Hilbert space with uniform eigenvalues.

3.3 Conclusion

We have studied the interferometric setup of Hardy's paradox from the point of view of the structure of the forward-scattered waves when the beam splitters of the scheme are considered as scattering centers. In the original setup, we have found that the forward-scattered wave is not of a product structure, and the forward-scattered wave for both beam splitters is not simply a linear combination of that of the two beam splitters. It is interesting to note that the forward-scattered wave has zero amplitude for the photon possibly generated in the system, which illustrates the relation between Hardy's paradox and interaction-free measurement. It would be interesting to systematically clarify the exact role of the entanglementlike structure of forward-scattered waves in interferometric setups with optionally placeable beam splitters, considering beam splitters as scattering centers. Altogether our result further illustrates that approaches which are successful in well explaining single-particle quantum phenomena (such as interaction-free measurement) do not necessarily provide an intuitive explanation of multipartite phenomena, they rather reveal that they are inherently quantum mechanical in a sense. Nevertheless the behavior of the so-calculated forward-scattered wave does not seem to be accidental and might prove to be a good tool for the analysis of such setups.

Chapter 4

Forward-scattered wave analysis of an optical Hardy-like setup

In this Chapter we analyze a photon interferometric scenario which is directly similar to that of the gedanken experiment of Hardy, where the annihilation of the particle-antiparticle pair is replaced by the interference of the two photons on a beam splitter. We discuss its relation to Hardy's paradox. We calculate the forward-scattered waves of the output beam splitters for this setup and analyze their entanglement-like structure.

In the previous chapter we have pointed out (see also: [33]) that the gedanken experiment of Hardy can be studied in the framework of scattering theory as applied by Geszti [30] to interaction-free measurement. Calculating the so-called forward scattered waves for the replaceable beam splitters of the setup, we find that they exhibit an entanglement-like structure. It is of some interest to seek for other schemes of the same kind, to obtain a deeper understanding of this entanglement-like structure.

In a possible experimental realization of Hardy's setup one has to face an obstacle that interferometry with a particle and an antiparticle is beyond any available experimental technology. As in case of many fundamental issues of quantum mechanics, optics, especially photon interferometry provides a proper playground for experimental realization. However, the annihilation of two photons is not viable in experiments with photons, hence, some modifications of the scenario is needed. The experimental

tests of the paradox by Lundeen and Steinberg [28] and independently by Yokota et al. [29] a modified version of the original setup in which weak measurements are carried out for identifying photon paths instead of considering simply detector click correlations as in the original gedanken experiment.

In this chapter we consider Hardy's original interferometer, except some relevant modification: the particles entering the setup are both photons, and the point where the electron and positron can annihilate each other in the original setup, the photons can interfere on a symmetric beam splitter, introducing the coupling between the two Mach-Zehnder interferometers. The detectors are considered to be photon counters. We call this setup a „Hardy-like” setup, since it obviously does not realize Hardy's paradox. In this chapter we leave open the question whether it is capable of violating local realism in any way (maybe different from Hardy's idea) or not. Instead, as a preliminary study, we study the forward-scattered waves and entanglement-like structure in the spirit of Ref. [33]. We find some similarities in the behavior of the two setups, however, the quantities characterizing entanglement are different.

4.1 The optical Hardy-like setup

The optical Hardy-like setup is depicted in Fig. 4.1. It consists of two Mach-Zehnder interferometers. Numbers indicate the modes of the interferometers, while letters denote modes before and after the photons cross the different beam splitters. As mentioned in the introduction, it is similar to Hardy's gedanken experimental setup except that the particles entering are both photons, and at point P, where the electron and the positron can annihilate each other, a symmetric beam splitter (denoted by BS_{14}^{bc} in Fig. 4.1) is placed.

In the whole setup we consider symmetric beam splitters, which transform their input modes ($\hat{a}_{in,1}$ and $\hat{a}_{in,2}$) to output modes according to the following transformation:

$$\hat{a}_{out,1} \rightarrow \frac{1}{\sqrt{2}}(\hat{a}_{in,1} + i\hat{a}_{in,2}), \quad (4.1)$$

$$\hat{a}_{out,2} \rightarrow \frac{1}{\sqrt{2}}(\hat{a}_{in,2} + i\hat{a}_{in,1}). \quad (4.2)$$

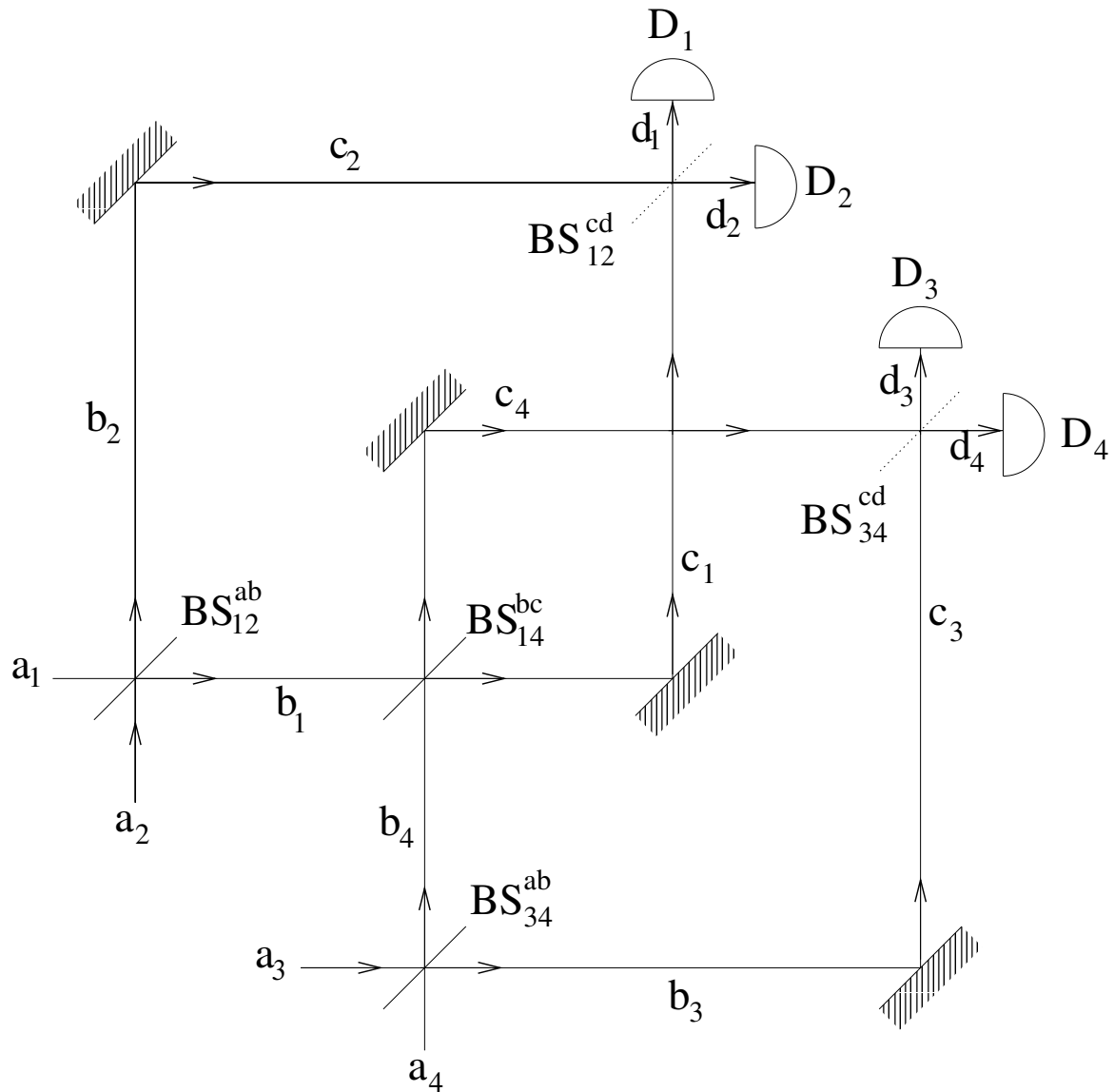


Figure 4.1: The interferometric setup in argument. Two Mach-Zehnder interferometers, coupled by the beam-splitter BS_{14} (as opposed to Hardy's paradox where there is simply a possibility of annihilation of a particle and antiparticle contained by the different interferometers). The other two beam-splitters are optionally replaceable, the detectors are photon number resolving ones.

This implies that the transformation of the two-mode photon states, in photon number representation, for the input states relevant for the present setup transform as

$$|01\rangle \rightarrow \frac{1}{\sqrt{2}}(|01\rangle + i|10\rangle), \quad (4.3)$$

$$|10\rangle \rightarrow \frac{1}{\sqrt{2}}(|10\rangle + i|01\rangle), \quad (4.4)$$

$$|02\rangle \rightarrow \frac{1}{2}(|02\rangle + \sqrt{2}i|11\rangle - |20\rangle), \quad (4.5)$$

$$|20\rangle \rightarrow \frac{1}{2}(|20\rangle + \sqrt{2}i|11\rangle - |02\rangle), \quad (4.6)$$

$$|11\rangle \rightarrow \frac{i}{\sqrt{2}}(|20\rangle + |02\rangle). \quad (4.7)$$

In the studied setup, we consider situations similar to those considered by Hardy in the gedanken experiment: some of the output beam splitters are either replaced (or equivalently, made completely transmissive) or not. The four possible arrangements are:

- i. every beam splitter is in place,
- ii. BS_{12}^{cd} is removed,
- iii. BS_{34}^{cd} is removed,
- iv. BS_{12}^{cd} and BS_{34}^{cd} are removed.

For these arrangements we find the following output states, respectively. (They are given in the photon number basis for the four modes, the order of the photon numbers in the kets follows the numbering of modes in Fig. 4.1) The state with all the beam splitters in place reads

$$\begin{aligned} |out1\rangle = & \frac{1}{8} \left[-i(\sqrt{2} + 1)\sqrt{2}(|2000\rangle + |0002\rangle) \right. \\ & + i(1 - \sqrt{2})\sqrt{2}(|0200\rangle + |0020\rangle) \\ & + 2(|1100\rangle + |0011\rangle) + 2i(|1010\rangle + |0101\rangle) \\ & \left. - 2(1 + \sqrt{2})|1001\rangle + 2(1 - \sqrt{2})|0110\rangle \right], \quad (4.8) \end{aligned}$$

the state without BS_{12}^{cd} is

$$\begin{aligned}
|out2\rangle = & \frac{1}{4} \left[-i\sqrt{2}|2000\rangle - \sqrt{2}|1100\rangle + i|1010\rangle + |0011\rangle \right. \\
& - |1001\rangle + (\sqrt{2} - 1)|0110\rangle + i(\sqrt{2} + 1)|0101\rangle \\
& \left. - i\frac{\sqrt{2} - 1}{2}\sqrt{2}|0020\rangle - i\frac{\sqrt{2} + 1}{2}\sqrt{2}|0002\rangle \right]. \tag{4.9}
\end{aligned}$$

Naturally the state without BS_{34}^{cd} is very similar to the latter one, because they are symmetric to each other:

$$\begin{aligned}
|out3\rangle = & \frac{1}{4} \left[-i\sqrt{2}|0002\rangle - \sqrt{2}|0011\rangle + i|0101\rangle + |1100\rangle \right. \\
& - |1001\rangle + (\sqrt{2} - 1)|0110\rangle + i(\sqrt{2} + 1)|1010\rangle \\
& \left. - i\frac{\sqrt{2} + 1}{2}\sqrt{2}|2000\rangle - i\frac{\sqrt{2} - 1}{2}\sqrt{2}|0200\rangle \right]. \tag{4.10}
\end{aligned}$$

The state without the any of the output beam splitters of the interferometers (i.e. without BS_{12}^{cd} and BS_{34}^{cd}) reads

$$\begin{aligned}
|out4\rangle = & \frac{1}{2} \left[\frac{i}{\sqrt{2}}(|1010\rangle + |0101\rangle - |2000\rangle - |0002\rangle) \right. \\
& \left. |0110\rangle - \frac{1}{\sqrt{2}}(|1100\rangle + |0011\rangle) \right]. \tag{4.11}
\end{aligned}$$

For sake of comparison it is interesting to recall the states which were to emerge in the case of the electron and positron in Hardy's setup. These states are (c.f. Ref. [33]):

$$\begin{aligned}
|out1\rangle = & \frac{1}{4}(-2|0000\rangle - |0110\rangle + i|0101\rangle \\
& + i|1010\rangle - 3|1001\rangle), \\
|out2\rangle = & \frac{\sqrt{2}}{4}(-\sqrt{2}|0000\rangle + i|0101\rangle \\
& + 2i|1010\rangle - |1001\rangle), \\
|out3\rangle = & \frac{\sqrt{2}}{4}(-\sqrt{2}|0000\rangle + 2i|0101\rangle \\
& + i|1010\rangle - |1001\rangle), \\
|out4\rangle = & \frac{1}{2}(-|0000\rangle + |0110\rangle + i|0101\rangle + i|1010\rangle). \tag{4.12}
\end{aligned}$$

In these formulae, $|0000\rangle$ refers to the vacuum state in the subspace of the electron and positron. This is the case of annihilation. In the other four states we have an electron and a photon in the respective

modes. Even though these are Fermions, there is exactly one of each, hence, these number states can be compared with the Bosonic ones with photons.

It appears that the states in Eq. 4.12 are different from those in Eqs. 4.8-4.11. There is no vacuum state in the optical setup. There are however some doubly occupied states which would be impossible in the Fermionic case, and also, there are cases in which both photons end up on the same side. To obtain a Hardy-like scenario we omit these states. Physically this can be done by a kind of local filtering: if a state with two photons in total (n.b. we assume photon-counting detectors) is detected on either side, the experiment is considered as invalid. Mathematically we omit these summands and renormalize the states. As a result we get states similar to those in Eq. 4.12, however, still with other coefficients. It is clear that the Hardy-like setup does not realize Hardy's paradox directly, with the omission of the unsuitable states. Nevertheless, one may analyze the forward scattered waves and the output probabilities. While we leave the latter question open in this study, we continue with the former.

4.2 Forward scattering

In the case of the setup which can be seen in Fig. 4.1, forward-scattered waves can be calculated just like that we explained in Sec. 3.2.

This time – just as in Sec. 3.2 – we have three possibilities for calculating forward scattering amplitudes. In each case, the reference is the absence of both beam splitters, BS_{12}^{cd} and BS_{34}^{cd} , but we can decide which of the beam splitters (BS_{12}^{cd} or BS_{34}^{cd}) are in their place. Being the beam splitters local objects, we would think that the forward-scattered wave generated by either of them does not influence that of the other beam splitter. As we saw in Sec. 3.2, we will see that this is not the case, even in this setup.

We may now calculate three forward-scattered waves (FSWs). They are calculated by subtracting the state of arrangement (iv) from the ones of arrangements (i), (ii) and (iii), and omitting the basis states which are not suitable for the scenario as described in the previous Section. The resulting FSWs are

the following:

$$\begin{aligned}
|FSW1\rangle &= c_1(|out1\rangle - |out4\rangle) = \\
&= \frac{1}{12}[i(1 - \sqrt{2})(|1010\rangle + |0101\rangle) \\
&\quad - (1 + \sqrt{2})(|1001\rangle + |0110\rangle)], \\
|FSW2\rangle &= c_2(|out2\rangle - |out4\rangle) \\
&= \frac{1}{8(2 - \sqrt{2})}[i(1 - \sqrt{2})|1010\rangle - |1001\rangle \\
&\quad + (\sqrt{2} - 3)|0110\rangle + i|0101\rangle], \\
|FSW3\rangle &= c_3(|out3\rangle - |out4\rangle) = \\
&= \frac{1}{8(2 - \sqrt{2})}[i|1010\rangle - |1001\rangle \\
&\quad + (\sqrt{2} - 3)|0110\rangle + i(1 - \sqrt{2})|0101\rangle], \tag{4.13}
\end{aligned}$$

where c_i ($i=1,2,3$) are constant normalization factors. As in Sec. 3.2, we consider the entanglement-like structure in the FSWs in Eq. 4.13. We talk about entanglement-like structure since the FSWs do not describe a physical system. Yet the fact that they are not separable is conjectured to relate to quantum correlations.

At the exit beam splitters, we may consider our system as that of two quantum bits, with two orthogonal states which are represented by the output spatial modes of the beam splitters. We do not consider the whole description of the system but the forward-scattered waves only. Due to this fact, we can now calculate the concurrences of the different forward-scattered waves using the Wootters formula [1] (presented in Section 1.2). After calculating, we get the following results:

$$\begin{aligned}
C_1 &= 1, \\
C_2 &= C_3 = 1/2. \tag{4.14}
\end{aligned}$$

In comparison with the original Hardy setup, where we have $C_1 = 1$, $C_2 = C_3 = 2/3$, we see that there are some similarities between the two scenarios: the maximal entanglement for the first FSW, and the equality of the entanglement for the other two, which is an obvious consequence of the symmetry of the setup. If the present setup could provide some violation of local realism, in the

present form, one might conjecture that it is related to the entanglement-like structure of the second two FSWs. However, the fact that the concurrence is below $2/3$ in the present setup might suggest that this is not the case. We leave the decision for further consideration.

In the present study we gave another particular example of the approach in [33], which serves as another example of its applicability.

4.3 Conclusion

We have analyzed an optical setup similar to that of the Hardy paradox along the same lines of thought which was applied to the original scenario in the previous Section. We have found that apart from the difference of certain details, there is a similarity between the behaviors of the forward-scattered waves in the two scenarios.

Chapter 5

Summary

In my thesis I have presented my results related to two main topics. One of them was the entanglement manipulation capabilities of the universal covariant quantum cloner or quantum processor circuit for quantum bits, and the other one was a similarly interesting theme where I analyzed Hardy's paradox from the point of view of scattering theory. My work belongs to the area of quantum information theory. The phenomenon of quantum entanglement plays a fundamental role in both of the mentioned topics.

Using certain quantifications of entanglement I have analyzed the entanglement manipulation capabilities of the universal covariant quantum cloner or quantum processor circuit for quantum bits. In the analysis the cloning a member of a bipartite or a genuine tripartite entangled state of quantum bits was considered. In case of bipartite states question to be answered was how much of bipartite entanglement "remains" between the original qubit and the other member of the pair, and how much of it is "transferred" to the clone when varying the cloning fidelity. I found that for bipartite pure entangled states a nontrivial behavior of concurrence appears. I have also studied the situation for cloning a member of GHZ entangled states, which are genuine tripartite states. The question here is the quantification of bipartite entanglements which are available via measurements on certain subsystems. I found that the partial extraction of bipartite entanglement can be achieved. These procedures can be useful in quantum communication and computation protocols.

The study of Hardy's paradox from the point of view of scattering theory was motivated by the fact that this approach was useful for the understanding of interaction-free measurement, which is a similar setup. I have calculated the forward-scattered waves generated by the beam splitters, which are replaceable in the gedanken experiment. I pointed out that these two-mode waves appear to have an entanglement-like structure, reflecting the quantum nature of the phenomenon.

Since there is a photon interferometric scenario which is directly similar to that of the gedanken experiment of Hardy, where the annihilation of the particle- antiparticle pair is replaced by the interference of the two photons on a beam splitter, it was interesting to analyze its relation to Hardy's paradox. I calculated the forward-scattered waves of the output beam splitters for this setup and analyzed their entanglement-like structure. I found similarities with the original paradox.

My new scientific results are enumerated below. The list of scientific publications concerning these results can be found in a separate Chapter.

1. I have shown that when using a universal covariant quantum cloning circuit to clone a member of an entangled pair of qubits, a very specific behavior of the entanglement of the qubits appears in its dependence on the cloning fidelity. The main feature is that behavior of the entanglement between the not cloned part of the pair and the cloned one is repeated in the entanglement of certain ancillae, and so is that of the not cloned qubit and the clone, provided that the original qubit pair was maximally entangled initially. My thesis includes the detailed description of the behavior of entanglement. Additionally, I showed that analyzed the cloning of an element of the GHZ state. I have shown that the universal quantum cloning circuit facilitates the partial extraction of bipartite entangled resources from a genuine tripartite entangled resource. I gave a detailed analysis of the entanglement behavior, including the relation to Coffman-Kundu-Wootters inequalities.

In summary, I have shown that the universal quantum cloning circuit (or quantum processor) for qubits can be used as an entanglement manipulator as well. It can perform entanglement manipulations which are potentially applicable in quantum information processing [I].

2. I have studied the interferometric setup of Hardy's paradox from the point of view of the structure of the forward-scattered waves when the beam splitters of the scheme are considered as scattering

centers. I showed that in the original setup, the forward-scattered wave is not of a product structure, and the forward-scattered wave for both beam splitters is not simply a linear combination of that of the two beam splitters. The forward-scattered wave has zero amplitude for the photon possibly generated in the system, which illustrates the relation between Hardy's paradox and interaction-free measurement. This approach might prove to be a good tool for the analysis of such setups[II].

3. I have investigated a realizable experimental setup which is directly similar to the one that was dealt with in the previous point. In this setup the role of particle-antiparticle annihilation was played by the interference of two photons on the beam splitter. I have calculated the respective forward-scattered waves. Though the values of the quantities featuring the entanglement were not equal to the values obtained in the case of Hardy's original gedanken experiment, the behaviour of the two setups showed similarities[III].

Chapter 6

Összefoglalás

(Summary in Hungarian)

Disszertációmban két témával kapcsolatos eredményeimet mutattam be. Ezek egyikében az univerzális kovariáns kvantumklónozó, vagy kvantumprocesszor alkalmazását vizsgáltam összefonódott állapotok manipulálására. A másik téma a Hardy-paradoxon egyfajta szóráselméleti elemzése. A bemutatott munka a kvantum-információelmélet területéhez kötődik. Az említett témakörökben végzett kutatás során végig alapvető jelentőséggel bírt a kvantumos összefonódás jelensége.

Az összefonódás bizonyos számszerű jellemzőinek használatával megvizsgáltam az összefonódás optimális univerzális aszimmetrikus kovariáns kvantum klónozóval (vagy kvantumprocesszorral) való manipulálhatóságát kvantumbitek esetében. Kétrés�ű állapotok esetén az volt a kérdés, hogy a klónozás hűségének függvényében mennyi összefonódás „marad” a pár másik tagja és klónozott tagja közt, és mennyi „megy át” a klónra. Azt találtam, hogy a kétrés�ű összefonódás, konkurenciában mérve, nemtriviális viselkedést mutat. Megvizsgáltam a GHZ állapot esetét is, amely inherensen háromrés�ű összefonódást mutat. Itt a feladat azon kétrés�ű összefonódások karakterizálása volt, amelyek a különböző részrendszereken végzett mérésekkel állíthatók elő. Azt találtam, hogy az összeállítás alkalmas a háromrés�ű összefonódás részleges kétrés�űvé alakítására. Ezek az eljárások hasznosak lehetnek különféle kvantuminformációs és kvantum számítási protokollokban.

A Hardy-paradoxon szóráselmélet nézőpontjából való vizsgálatát az a tény motiválta, hogy ez a hozzáállás egyszer már gyümölcsözőnek bizonyult a Hardy-paradoxon kísérleti elrendezésével nagy hasonlóságot mutató kölcsönhatás-mentes mérés elméleti háttérének megvilágításakor. Az elemzés során a Hardy-féle gondolkísérlet berendezésében opcionálisan kivehető illetve betehető nyalábosztók előreszórt hullámait kiszámítva megmutattam, hogy az említett kétrészű állapotvektorok összefonódott szerkezetűek, ami a jelenség erősen kvantumos természetére utal.

Tekintve, hogy létezik egy, a Hardy-féle gondolkísérletben szereplő kísérleti elrendezéshez nagyon hasonló foton interferometriai berendezés, ahol az eredeti Hardy-változatban említett részecske-antirészecske annihiláció szerepét a nyalábosztón találkozó fotonok interferenciája veszi át, érdekes volt megvizsgálni e kísérlet Hardy-paradoxonhoz való viszonyulását, mégpedig az adott kísérleti elrendezés megfelelő nyalábosztóihoz tartozó előreszórt hullámok elemzésén keresztül. Ezek szerkezetében az eredeti paradoxon esetéhez hasonló tulajdonságokat találtam.

Új tudományos eredményeimet az alábbi pontokban foglalom össze. Az eredményeket taglaló tudományos közlemények felsorolása a "List of related publications" cím alatt található.

1. Megmutattam, hogy ha egy kezdetben maximálisan összefonódott kvantumbit pár egyik tagját klónozzuk, a kvantumbitek összefonódása sajátos viselkedést mutat. Ennek fő jellemzője az, hogy a klónozás művelete után az eredeti kvantumbit pár két tagja – a nem klónozott és a klónozott – közötti összefonódás éppen úgy viselkedik, mint ahogy az az egyes segéd kvantumbitek jellemző összefonódás esetében megfigyelhető. Ugyanez tapasztalható a nem klónozott kvantumbit és a klón közötti összefonódás tekintetében, melynek viselkedése a klónozott kvantumbit és a másik segéd kvantumbit közötti összefonódáséval mutat teljes egyezést. Az összefonódás viselkedésének részletes leírását tartalmazza a disszertáció.

Ugyanezen elemzés kapcsán megmutattam azt is, hogy egy GHZ állapot egyik tagjának klónozásakor, az kvantumklónozó eszköz lehetővé teszi a kétrészű összefonódott erőforrások eredetileg teljesen háromrészű összefonódott erőforrásból való részleges kivonását. Az összefonódás viselkedéséről részletes elemzést adtam ebben az esetben, a Coffman-Kundu-Wootters egyenlőtlenségeket is felhasználva.

Összefoglalva: megmutattam, hogy az univerzális kvantumklónozó (más néven: kvantum processzor) az összefonódás manipulálásának is hasznos eszköze, ezáltal ily módon is hasznos lehet a kvantuminformáció feldolgozás területén [I].

2. Megvizsgáltam a Hardy-paradoxonban szereplő interferometriai berendezést, annak nyálábosztói-ra, mint szóró centrumokra tekintve, az előreszórt hullámok szerkezetéből kiindulva. Kimutattam, hogy az eredeti elrendezésben az előreszórt hullám nem szorzat-szerkezetű, továbbá azt is, hogy a két nyálábosztó előreszórt hulláma nem állítható elő az egyedi nyálábosztók előreszórásainak lineárkombinációjaként. Az előreszórt hullám nulla nagyságú valószínűségi amplitúdót tartalmaz a rendszerben potenciálisan létrejövő foton esetére vonatkozólag, ami a Hardy-paradoxon és a kölcsönhatás-mentes mérés közötti viszonyt illusztrálja. Ez a hozzáállás hasznosnak bizonyulhat a hasonló elrendezések elemzésekor [II].
3. Megvizsgáltam egy, az előző pontban tárgyalthoz hasonló, ténylegesen kivitelezhető kísérleti berendezést, ahol a Hardy-paradoxonban vázolt elrendezésben szereplő részecske-antirészecske annihiláció helyét két foton, nyálábosztón történő interferenciája vette át, ezúton csatolván a két, interferométert. Kiszámítottam a kimenet nyálábosztóinak előreszórt hullámait, s az előző pontban említett módszert alkalmazva megvizsgáltam azok összefonódás-szerű szerkezetét. Noha az összefonódást jellemző mennyiségek nem egyeztek az eredeti gondolkísérlet esetén kapott értékekkel, a két elrendezés viselkedése mutatott hasonlóságokat [III].

List of related publications

- I. L. Szabó, M. Koniorczyk, P. Adam, and J. Janszky: *Optimal universal asymmetric covariant quantum cloning circuits for qubit entanglement manipulation* Phys. Rev. A **81**, 032323 (2010).
- II. M. Koniorczyk, L. Szabó and P. Adam: *Hardy's paradox and the entanglementlike structure of forward-scattered waves*, Phys. Rev. A **84**, 044102 (2011).
- III. P. Adam, L. Szabó, M. Mechler, M. Koniorczyk: *Forward-scattered wave analysis of an optical Hardy-like setup*, Phys. Scr. **T147**, 014001/1-4 (2012).

Acknowledgements

Though I tried to do my best during my fellowship, I would not have realized these fruitages without the help of my supervisor whose name is Mátyás Koniorczyk. Hereby I would like to demonstrate my acknowledgement for his professional help and caring encouragement. I am in hock to my wife, too. She helped me to work on this thesis by ensuring the relaxed background.

Bibliography

- [1] W. K. Wootters, Phys. Rev. Lett. **80**, 2245 (1998).
- [2] V. Coffman, J. Kundu, and W. K. Wootters, Phys. Rev. **61**, 052306 (2000).
- [3] W. K. Wootters and W. H. Zurek, A single quantum cannot be cloned, Nature **299**, 802 (1982)
- [4] R. F. Werner, Phys. Rev. A **58**, 1827 (1998).
- [5] V. Bužek and M. Hillery, Phys. Rev. A **54**, 1844 (1996).
- [6] N. J. Cerf, Phys. Rev. Lett. **84**, 4497 (2000).
- [7] N. J. Cerf, J. Mod. Opt. **47**, 187.209 (2000).
- [8] V. Scarani, S. Iblisdir, N. Gisin, and A. Acín, Rev. Mod. Phys. **77**, 1225 (2005).
- [9] V. Bužek, S. L. Braunstein, M. Hillery, and D. Bruß, Phys. Rev. A **56**, 3446 (1997).
- [10] S. Braunstein, V. Bužek, and M. Hillery, Phys. Rev. A **63**, 052313 (2001).
- [11] M. A. Nielsen and I. L. Chuang, Phys. Rev. Lett. **79**, 321 (1997).
- [12] M. Hillery, V. Bužek, and M. Ziman, Phys. Rev. A **65**, 022301 (2002).
- [13] J. Novotný, G. Alber, and I. Jex, Phys. Rev. A **71**, 042332 (2005).
- [14] L.-P. Lamoureux, P. Navez, J. Fiurášek, and N. J. Cerf, Phys. Rev. A **69**, 040301 (2004).
- [15] E. Karpov, P. Navez, and N. J. Cerf, Phys. Rev. A **72**, 042314 (2005).

-
- [16] V. Bužek and M. Hillery, *Phys. Rev. Lett.* **81**, 5003 (1998).
- [17] S. Adhikari, B. Choudhury, and I. Chakrabarty, *J. Phys. A-Math. Gen.* **39**, 8439 (2006).
- [18] I. Chakrabarty and B. S. Choudhury, *Int. J. Quantum Inf.* **7**, 559 (2009).
- [19] S. Adhikari and B. S. Choudhury, *Phys. Rev. A* **74**, 032323 (2006).
- [20] I. Ghiu and A. Karlsson, *Phys. Rev. A* **72**, 032331 (2005).
- [21] S. Bandyopadhyay and G. Kar, *Phys. Rev. A* **60**, 3296 (1999).
- [22] M. MiCuda, M. Ježek, M. Dušek, and J. Fiurašek, *Physical Review A (Atomic, Molecular, and Optical Physics)* **78**, 062311 (2008).
- [23] D. M. Greenberger, M. A. Horne, and A. Zeilinger, *Physics Today* **46**, 22 (1993).
- [24] A. Einstein, B. Podolsky, and N. Rosen, *Phys. Rev.* **47**, 777 (1935).
- [25] J. S. Bell, *Physics (NY)* **1**, 195 (1965).
- [26] J. F. Clauser, M. A. Horne, A. Shimony, and R. A. Holt, *Phys. Rev. Lett.* **23**, 880 (1969).
- [27] L. Hardy, *Phys. Rev. Lett.* **68**, 2981 (1992).
- [28] J. S. Lundeen and A. M. Steinberg, *Phys. Rev. Lett.* **102**, 020404 (2009).
- [29] K. Yokota, T. Yamamoto, and M. K. N. Imoto, *New J. Phys.* **11**, 033011 (2009).
- [30] T. Geszti, *Phys. Rev. A* **58**, 4206 (1998).
- [31] M. Koniorczyk and V. Bužek, *Phys. Rev. A* **71**, 032331 (2005).
- [32] T. Laustsen, F. Verstraete, and S. J. van Enk, *Quantum Inf. Comput.* **3**, 64 (2003).
- [33] M. Koniorczyk, L. Szabó and P. Adam, *Phys. Rev. A* **84**, 044102 (2011).
- [34] A. C. Elitzur and L. Vaidman, *Found. Phys.* **23**, 987 (1993); L. Vaidman, *Quantum Opt.* **6**, 119 (1994).